AIMS Mathematics, 11(3): 6050–6079.
DOI: 10.3934/math.2026251
Received: 16 October 2025
Revised: 25 February 2026
Accepted: 04 March 2026
Published: 10 March 2026

https://www.aimspress.com/journal/Math

Research article

Dynamics of solitary waves in the stochastic complex coupled Kuralay model

Sadia Yasin[1], **Beenish**[2], **Salma Trabelsi**[3] **and Meraa Arab**[3,*]

[1] Department of Mathematics, University of Okara 56130, Punjab, Pakistan
[2] Department of Mathematics, Quaid-I-Azam University 45320, Islamabad, Pakistan
[3] Department of Mathematics and Statistics, College of Science, King Faisal University, Al Ahsa 31982, Saudi Arabia

* **Correspondence:** Email: marab@kfu.edu.sa.

Abstract: In this article, we study the stochastic complex coupled Kuralay model, which possesses some applications in various fields, including physics, biology, and engineering, to obtain new solitary wave solutions. The explicit analytical solutions are obtained by using the Sardar subequation method, which helps to illuminate the dynamics of oscillators under random (noisy) effects. The integration of the Wiener process along a given method is a precise approximation of the stochastic behavior of the system. The proposed strategy enables the derivation of several exact solitary wave solutions under stochastic conditions, including bright, dark, and singular wave profiles. More significantly, the obtained solutions are also represented by 3D surface and contour plots that clearly show how solitary waves change and evolve when noise is introduced. Other stochastic models in physics and engineering can use the proposed approach to understand the workings of complex systems.

Keywords: Sardar sub-equation method; stochastic complex coupled Kuralay model; solitary wave solutions; Wiener process; multiplicative noise; exact solutions
Mathematics Subject Classification: 26A48, 26A51, 33B10, 37K40, 39B62

List of Abbreviations

PDEs Partial Differential Equations

NLPDEs Nonlinear Partial Differential Equations

CCK Complex Coupled Kuralay

CKM Coupled Kuralay Model

SSEM Sardar Subequation Method

ODEs Ordinary Differential Equations

SPDEs Stochastic Partial Differential Equations

List of Symbols

i Imaginary unit ($i^2 = -1$)

t Time variable

x Spatial variable

$\mathbb{U}(x,t)$ First complex wave function

$Q(x,t)$ Second wave function

$M(\xi)$ Amplitude function for $\mathbb{U}(x,t)$

γ Noise intensity parameter

$W(t)$ Wiener process (standard Brownian motion)

ξ Traveling wave variable: $\xi = sx + \eta t$

s Wave number parameter

η Wave speed parameter

v Spatial frequency parameter (appears in phase)

κ Temporal frequency parameter (appears in phase)

$\wp$ Phase constant

M', M'' First and second derivatives of M with respect to ξ

$\mathbb{U}_t$, $\mathbb{U}_x$, $\mathbb{U}_{xt}$ Partial derivatives of $\mathbb{U}$ with respect to t, x, and mixed

e Exponential function $\exp(\cdot)$

1. Introduction

Partial differential equations (PDEs) are powerful mathematical tools used to describe the behavior of different physical phenomena in physics, engineering, finance, and biology, among others. PDEs are effective in modeling difficult systems in which the amounts change over both distance and time. PDEs play a crucial role in modeling and predicting heat diffusion, fluid flows, magnetic fields, and waves [1]. They present a way of writing the basic rules governing the world as a when whole concerning preservation laws, including laws of movement, in a form that is solvable using calculus or through computer programs.

Nonlinear partial differential equations (NLPDEs) are a set of mathematical models that describe several phenomena in biology, chemistry, and physics, among other disciplines [2, 3]. Although both

linear and nonlinear PDEs share the properties of homogeneity and superposition, nonlinear PDEs are more complicated since the solutions do not linearly depend on their independent variables and derivatives. This nonlinearity poses a great challenge, both when the theory behind the equations is to be analyzed and when trying to solve the equations using a numerical method [4]. These equations cannot be explicitly solved in closed forms of simple formulas as linear equations, and are therefore to be either investigated by higher mathematics methods such as the methods of variation parameters and characterization or computed using computer algorithms under numerical methods. The perturbation theory [5], variational methods [6] and numerical simulations [7] are some approaches that help one understand how nonlinear systems behave according to PDEs.

Solitons play a important role in different areas, including fluid mechanics and nonlinear optics, and help us realize complicated procedures and facilitate far-reaching information transfer. They are steady wave packets that move at a fixed velocity without changing the shape or acceleration [8]. Such solutions exist in nonlinear equations such as Korteweg-de Vries and nonlinear Schrödinger equations [9, 42], because these equations have a special balance between dispersion and nonlinearity. Inverse scattering transform [11] and Hirota's method [12] are mathematical techniques to find such solutions which show the complex behavior of nonlinear systems.

Stochastic procedures and Brownian motion are basic tools to demonstrate irregularity and disorder in development fields. In essence, a stochastic procedure consists of random variables which change through time. The Wiener procedure, also known as Brownian motion, represents random movements with continuous traces and disjoint phases [13]. In many cases, researchers have employed the Wiener process noise, which follows a Gaussian distribution in various fields such as finance and engineering, to create and evaluate systems that experienced irregular changes. These mathematical suggestions provide useful details in complex systems controlled by ambiguity.

The complex coupled kuralay (CCK) model is a mathematical framework used in the study of complex systems, particularly in fields such as ecology, epidemiology, and social dynamics. Named after its author, Almaz Kuralay, this model forms upon the traditional coupled oscillator models to simulate relations between objects in a system that show both linear and nonlinear dynamics [15, 16].

The integrable complex coupled kurulay system defined as follows [40]:

$$\begin{aligned} &i\mathbb{U}_t - \mathbb{U}_{xt} - Q\mathbb{U} = 0,\\ &iS_t + S_{xt} + Q\mathbb{U} = 0,\\ &Q_x + 2f^2(S\mathbb{U})_t = 0, \end{aligned} \tag{1.1}$$

where Q is a potential real function, and $\mathbb{U}(x,t)$ is a complex function. By taking the assumption, $f = 1$, $S = n\bar{\mathbb{U}}$ with $n = \pm 1$ (1.1) reduce to:

$$\begin{aligned} &i\mathbb{U}_t - \mathbb{U}_{xt} - Q\mathbb{U} = 0,\\ &Q_x - 2n(|\mathbb{U}|^2)_t = 0. \end{aligned} \tag{1.2}$$

The CCK model is an effective instrument to investigate some phenomena in various domains stretching from science to engineering. Particularly, it is used to in explain how soliton propagation occurs within optical fibers, as well as to determine solitons and rogue waves in fluid dynamics.

Equilibrium is also a vital component in optical fiber systems because it results in the creation of discrete optical pulses called solitons. The defining characteristic of these solitons is that they

are able to orbit their shape and speed without considerable bending or distortion. The CCK model is an important tool to study how solitons move across such media [18]. The Coupled Kuralay Model (CKM) has arose as a crucial analytical tool to investigate the complex examination of nonlinear waves, particularly where coupled-component dispersion and nonlinearity are balanced in multi-mode systems. Initially, the CKM founds its primary physical resonance in the study of optical pulse dynamics in birefringent fibers and the classification of electromagnetic waves in plasma physics [18]. Along with these classical applications, recent integrative approaches in research have seen the model improved to biological contexts, such as the rhythmic synchronization of molecular oscillators and the propagation of signals within microtubule structures, where the coupling describes the intricate interaction between varying chemical or electrical potentials [19]. By providing a rigorous mathematical description of these interactions, the CKM allows for the prediction of localized structures that are fundamental to modern communication systems and biophysical modeling. However, a significant limitation of, existing deterministic frameworks is their reliance on an idealized "closed-system" assumption, which ignores the unavoidable fluctuations inherent in real-world environments. In practice, phenomena such as thermal noise, background radiation, and microscopic impurities introduce a layer of randomness that can destabilize or fundamentally reshape solitary waves. By incorporating stochasticity through additive or multiplicative noise, this study addresses a critical research gap such as the transition from theoretical vacuum models to robust, "open-system" representations [20]. The given model enables us to analyze that how nonlinearity and dispersion affect the behavior of solitons.

Wiener process and white noise [21]

In the stochastic model, the Wiener process $W(t)$ for $t \geq 0$ is used to represent random perturbations. It satisfies the following properties: $W(0) = 0$; the increments $W(t_2) - W(t_1)$ for $t_2 > t_1$ are independent and normally distributed with mean zero and variance $t_2 - t_1$; and $W(t)$ is continuous for all $t \geq 0$. White noise is defined as the formal time derivative of $W(t)$ and is employed to model events with instantaneous, stochastic fluctuations in the system. This rigorous framework ensures that the stochastic differential equations are well-posed and can be interpreted in the Ito sense [35].

The following equation represents the stochastic complex coupled kurulay system:

$$\begin{aligned} &i\mathbb{U}_t - \mathbb{U}_{xt} - Q\mathbb{U} = \gamma \frac{d\mathbb{W}(t)}{dt}, \\ &Q_x + 2n(|\mathbb{U}|^2)_t = 0. \end{aligned} \tag{1.3}$$

Various methods have been established to examine the NLPDEs and to find soliton solutions, such as the ansatz method [45], the bilinear neural network method [22], the homotopy perturbation technique [23], the unified method [44], the $\left(\frac{1}{\phi(\zeta)}, \frac{\phi'(\zeta)}{\phi(\zeta)}\right)$ method [44], the modified simple equation and $exp(-\varphi(q))$ method [36], the exp-function method [24], the Laplace transform technique [43], the extended auxiliary equation method [25], the very popular compact finite difference method [26], the ϕ^6 model expansion method [14], the sine-Gordon expansion method [27], the modified $\left(\frac{G'}{G^2}\right)$ expansion method [37, 38], the variational method [28], Khater method [39], the bilinear method [29], the new extended direct algebraic method [33], the improved modified Sardar subequation [41], and the Kudryashov method [32]. However, these approaches often involve lengthy algebraic manipulations and complex transformations. In contrast, the Sardar sub-equation method provides a simpler and more

systematic framework, which allows us to derive a broader class of exact solutions with a reduced computational effort.

The Sardar Subequation Method (SSEM) [8] is a powerful analytical method of solving nonlinear ordinary differential equations (ODEs) used in the analysis of nonlinear problems. It is primarily useful because it is a simple approach that offers a systematic approach to manage nonlinear problems with the least amount of calculation. In contrast to other methods, the Sardar subequation method used in this work offers several distinct advantages. First, it provides a systematic and direct framework to construct exact analytical solutions for stochastic nonlinear systems without requiring linearization or perturbation approximations. Second, the method allows the incorporation of stochastic effects through a Wiener process, thus enabling an accurate representation of random fluctuations in the governing equations. Nevertheless, the approach can face difficulties with the selection of suitable substitutions to achieve successful linearization, and the convergence and applicability to highly oscillatory or irregular equations need to be considered. Despite these limitations, the SSEM remains a valuable tool to simplify and solve nonlinear ODEs in both analytical and numerical contexts.

This study is motivated by the critical need to understand stochastic effects within complex systems, which is essential to accurately expect their dynamic behaviors in real-world applications. Our research introduces a new application of the SSEM to the stochastic CCK model. By applying this method, we find exact soliton solutions that provide deep insights into wave propagation dynamics influenced by random fluctuations. This contribution not only advances the theoretical understanding of nonlinear PDEs, but also offers practical implications across different scientific and engineering disciplines. Future work could explore extending this methodology to more complex systems or integrating additional variables to further enhance the predictive capabilities and expand the applicability in various fields.

The paper is organized as follows: Section 1 introduces the model; Section 2 outlines the methodology; Section 3 presents the soliton solutions; Section 4 shows simulations; and Section 5 concludes the study.

2. Methodology (SSM) [41]

Consider the following PDE:

$$\mathbb{U}(m, m_x, m_t, m_y, m_z, m_{tt}, m_{xx}, m_{zz}, m_{yy}, ...) = 0, \tag{2.1}$$

where $\mathbb{U}$ is a polynomial function.
By adopting the traveling wave transformation:

$$\mathbb{U}(x,t) = M(\xi)\, e^{i(\nu x+\kappa t+\wp+\gamma \mathbb{W}(t)-\frac{1}{2}\gamma^2 t)}, \;\; \mathbb{Q}(x,t) = \mathbb{Q}(\xi) \;\; and \quad \xi = \eta t + sx, \tag{2.2}$$

we obtain the following ODEs:

$$\mathbb{Q}(M, M^{'}, M^{''}, M^{'''}, ...) = 0, \tag{2.3}$$

where $M = M(\xi)$, $M^{'} = \frac{dM}{d\xi}$, $M^{''} = \frac{d^2M}{d\xi^2}, \cdots$.
The solution of (2.3) is as follows:

$$M(\xi) = \sum_{j=0}^{D} \gamma_j \aleph^j(\xi). \tag{2.4}$$

The $\aleph^j$ where $j = 0, 1, 2, \cdots, D$ are coefficients with constant values, and $\aleph'(\xi)$ is defined as follows:

$$\aleph'(\xi) = \sqrt{\rho + h\aleph(\xi)^2 + \aleph(\xi)^4}, \tag{2.5}$$

where ρ and h are real numbers. The exact solutions of (2.1) described below.
Case $*$ **I**: If $h > 0$ and $\rho = 0$, then we have the following:

$$\aleph_1^{\pm}(\xi) = \pm\sqrt{-abh}\ sech_{ab}(\sqrt{h}\xi),$$
$$\aleph_2^{\pm}(\xi) = \pm\sqrt{abh}\ csch_{ab}(\sqrt{h}\xi),$$

where

$$sech_{ab}(\xi) = \tfrac{2}{ae^{\xi}+be^{-\xi}}, \quad csch_{ab}(\xi) = \tfrac{2}{ae^{\xi}-be^{-\xi}}.$$

Case $*$ **II**: If $h < 0$ and $\rho = 0$, then we have the following:

$$\aleph_3^{\pm}(\xi) = \pm\sqrt{-abh}\ sec_{ab}(\sqrt{-h}\xi),$$
$$\aleph_4^{\pm}(\xi) = \pm\sqrt{-abh}\ csc_{ab}(\sqrt{-h}\xi),$$

where

$$sec_{ab}(\eta) = \tfrac{2}{ae^{\iota\xi}+be^{-\iota\xi}}, \quad csc_{ab}(\xi) = \tfrac{2\iota}{ae^{\iota\xi}-be^{-\iota\xi}}.$$

Case $*$ **III**: If $h < 0$ and $\rho = \frac{h^2}{4}$, then we have the following:

$$\aleph_5^{\pm}(\xi) = \pm\sqrt{\frac{-h}{2}}tanh_{ab}\left(\sqrt{\frac{-h}{2}}\xi\right),$$
$$\aleph_6^{\pm}(\xi) = \pm\sqrt{\frac{-h}{2}}coth_{ab}\left(\sqrt{\frac{-h}{2}}\xi\right),$$
$$\aleph_7^{\pm}(\xi) = \pm\sqrt{\frac{-h}{2}}\left(tanh_{ab}(\sqrt{-2h}\xi) \pm \iota\sqrt{ab}\ sech_{ab}(\sqrt{-2h}\xi)\right),$$
$$\aleph_8^{\pm}(\xi) = \pm\sqrt{\frac{-h}{2}}\left(coth_{ab}(\sqrt{-2h}\xi) \pm \sqrt{ab}\ csch_{ab}(\sqrt{-2h}\xi)\right),$$
$$\aleph_9^{\pm}(\xi) = \pm\sqrt{\frac{-h}{8}}\left(tanh_{ab}(\sqrt{\frac{-h}{8}}\xi) + coth_{ab}(\sqrt{\frac{-h}{8}}\xi)\right),$$

where

$$tanh_{ab}(\xi) = \tfrac{ae^{\xi}-be^{-\xi}}{ae^{\xi}+be^{-\xi}}, \quad coth_{ab}(\xi) = \tfrac{ae^{\xi}+be^{-\xi}}{ae^{\xi}-be^{-\xi}}.$$

Case $*$ **IV**: If $h > 0$ and $\rho = \frac{h^2}{4}$, then we have the following:

$$\aleph_{10}^{\pm}(\xi) = \pm\sqrt{\frac{h}{2}}tan_{ab}\left(\sqrt{\frac{h}{2}}\xi\right),$$

$$\aleph_{11}^{\pm}(\xi) = \pm\sqrt{\frac{h}{2}}cot_{ab}\left(\sqrt{\frac{h}{2}}\xi\right),$$
$$\aleph_{12}^{\pm}(\xi) = \pm\sqrt{\frac{h}{2}}\left(tan_{ab}(\sqrt{2h}\xi) \pm \sqrt{ab}\ sec_{ab}(\sqrt{2h}\xi)\right),$$
$$\aleph_{13}^{\pm}(\xi) = \pm\sqrt{\frac{h}{2}}\left(cot_{ab}(\sqrt{2h}\xi) \pm \sqrt{ab}\ csc_{ab}(\sqrt{2h}\xi)\right),$$
$$\aleph_{14}^{\pm}(\xi) = \pm\sqrt{\frac{h}{8}}\left(tan_{ab}(\sqrt{\frac{h}{8}}\xi) + cot_{ab}(\sqrt{\frac{h}{8}}\xi)\right),$$

where

$$tan_{ab}(\xi) = -\iota\frac{ae^{\iota\xi}-be^{-\iota\xi}}{ae^{\iota\xi}+be^{-\iota\xi}}, \quad cot_{ab}(\xi) = \iota\frac{ae^{\iota\xi}+be^{-\iota\xi}}{ae^{\iota\xi}-be^{-\iota\xi}}.$$

By using (2.3)–(2.5) and , we obtain exact solutions of the SSM by Mathematica11.0.

3. Soliton solutions of Kuralay model

This section will describe the conversion of a PDE using a wave transformation and obtaining soliton solutions of the Kuralay model. By applying the wave transformation to the complex differential equation:

$$\mathbb{U}(x,t) = M(\xi)\,e^{\left(\gamma\mathbb{W}(t)+i(\nu x+\kappa t+\wp)-\frac{\gamma^2 t}{2}\right)}, \quad Q(x,t) = Q(\xi) \ \ and \quad \xi = \eta t + sx. \tag{3.1}$$

We have:

$$\begin{aligned}
\mathbb{U}_t &= (\eta M^{'} + i\kappa M)e^{\left(\gamma\mathbb{W}(t)+i(\nu x+\kappa t+\wp)-\frac{\gamma^2 t}{2}\right)},\\
\mathbb{U}_x &= (sM^{'} + i\nu M)e^{\left(\gamma\mathbb{W}(t)+i(\nu x+\kappa t+\wp)-\frac{\gamma^2 t}{2}\right)},\\
\mathbb{U}_{xt} &= (\eta sM^{''} + i\kappa sM^{'} + i\eta\nu M^{'} + i\nu\kappa M)e^{\left(\gamma\mathbb{W}(t)+i(\nu x+\kappa t+\wp)-\frac{\gamma^2 t}{2}\right)}.
\end{aligned} \tag{3.2}$$

Substitute the value of (3.1) and (3.2) into (1.3) to obtain the following:

$$i(\eta M^{'} + i\kappa M) - (\eta sM^{''} + i\kappa sM^{'} + i\eta\nu M^{'} - \nu\kappa M) - QM = 0, \tag{3.3}$$

and

$$sQ^{'} - 4n\eta MM^{'} = 0. \tag{3.4}$$

By integrating (3.4), we obtain the following:

$$Q = \frac{2n\eta M^2}{s} - \frac{\eta_1}{s}. \tag{3.5}$$

By substituting (3.5) into (3.3), we have the following:

$$i(\eta M^{'} + i\kappa M) - \left(\eta sM^{''} + i\kappa sM^{'} + i\eta\nu M^{'} - \nu\kappa M\right) - \left(\frac{2n\eta M^2}{s} - r\right)M = 0, \tag{3.6}$$

where $r = \frac{\eta_1}{s}$.
By separating the real and imaginary parts of (3.6),

$$M^{''} + \frac{(\kappa(1-v)-r)}{\eta s}M + \frac{2nM^3}{s^2} = 0, \tag{3.7}$$

and

$$(\eta - \kappa s - \eta v)M^{'} = 0. \tag{3.8}$$

The imaginary part (3.8) provides the following:

$$s = \frac{\eta(1-v)}{\kappa}. \tag{3.9}$$

Substitute the value of s into (3.7) to obtain the following ODE:

$$M^{''} + \frac{\kappa(\kappa(1-v)-r)}{\eta^2(1-v)}M + \frac{2\kappa^2 nM^3}{\eta^2(1-v)^2} = 0. \tag{3.10}$$

Balance the terms to get the homogenous constant $D = 1$, which reduces (2.4) into the following:

$$M(\theta) = \gamma_0 + \gamma_1 \aleph(\theta). \tag{3.11}$$

Substitute the value of (3.11) along (2.5) into (3.10) and gather all coefficients of the polynomial to obtain algebraic equations.

$$\begin{aligned}
&\aleph(\theta)^0 : \frac{2\gamma_0^3 n\kappa^2}{\eta^2(1-v)^2} - \frac{\gamma_0\kappa r}{\eta^2(1-v)} + \frac{\gamma_0\kappa^2}{\eta^2(1-v)} - \frac{\gamma_0\kappa^2 v}{\eta^2(1-v)},\\
&(\aleph(\theta)) : \frac{6\gamma_0^2\gamma_1 n\kappa^2}{\eta^2(1-v)^2} + \gamma_1 h - \frac{\gamma_1\kappa r}{\eta^2(1-v)} + \frac{\gamma_1\kappa^2}{\eta^2(1-v)} - \frac{\gamma_1\kappa^2 v}{\eta^2(1-v)},\\
&(\aleph(\theta))^2 : \frac{6\gamma_0\gamma_1^2 n\kappa^2}{\eta^2(1-v)^2},\\
&(\aleph(\theta))^3 : \frac{2\gamma_1^3 n\kappa^2}{\eta^2(1-v)^2} + 2\gamma_1.
\end{aligned} \tag{3.12}$$

We obtain the following:

$$\gamma_0 = 0; \quad \gamma_1 = \pm\frac{i\eta(v-1)}{\sqrt{n}\kappa}; \quad h = -\frac{\kappa(r+v\kappa-\kappa)}{\eta^2(v-1)}. \tag{3.13}$$

The exact solution of (1.3) can be obtained in a following way by using (3.13) with (3.11) and (3.5).
Case $*$ **I**: If $h > 0$, and $\rho = 0$, then we have the following:

$$\mathbb{U}_{1,1}^{\pm} = \pm\left[\left(\frac{i\eta(v-1)}{\sqrt{n}\kappa}\right)\left(\sqrt{\frac{-ab\kappa(r+v\kappa-\kappa)}{\eta^2(v-1)}}\right)\mathrm{Sech}_{\mathrm{ab}}\left(\sqrt{-\frac{\kappa(r+v\kappa-\kappa)}{\eta^2(v-1)}}(\xi)\right)\right]$$
$$e^{\left(\gamma\mathbb{W}(t)+i(\nu x+\kappa t+\varphi)-\frac{\gamma^2 t}{2}\right)},$$

$$Q_{1,1}^{\pm} = \pm\frac{1}{m}[-\eta_1 + 2\eta n\left(\frac{i\eta(v-1)}{\sqrt{n}\kappa}\right)^2\left(\sqrt{\frac{ab\kappa(r+v\kappa-\kappa)}{\eta^2(v-1)}}\right)^2$$

$$\mathrm{Sech}_{\mathrm{ab}}\left(\sqrt{-\frac{\kappa(r+v\kappa-\kappa)}{\eta^2(v-1)}}(\xi)\right)^2],$$

$$\mathbb{U}_{1,2}^{\pm} = \pm\left[\left(\frac{i\eta(v-1)}{\sqrt{n}\kappa}\right)\left(\sqrt{-\frac{ab\kappa(r+v\kappa-\kappa)}{\eta^2(v-1)}}\right)\mathrm{Csch}_{\mathrm{ab}}\left(\sqrt{-\frac{\kappa(r+v\kappa-\kappa)}{\eta^2(v-1)}}(\xi)\right)\right]$$

$$e^{\left(\gamma\mathbb{W}(t)+i(vx+\kappa t+\varphi)-\frac{\gamma^2 t}{2}\right)},$$

$$Q_{1,2}^{\pm} = \pm\frac{1}{m}[-\eta_1 + 2\eta n\left(\frac{i\eta(v-1)}{\sqrt{n}\kappa}\right)^2\left(\sqrt{-\frac{ab\kappa(r+v\kappa-\kappa)}{\eta^2(v-1)}}\right)^2$$

$$\mathrm{Csch}_{\mathrm{ab}}\left(\sqrt{-\frac{\kappa(r+v\kappa-\kappa)}{\eta^2(v-1)}}(\xi)\right)^2],$$

where

$$\xi = \eta t + sx, \qquad \frac{-ab\kappa(r+v\kappa-\kappa)}{\eta^2(v-1)} > 0, \qquad and \qquad \frac{-\kappa(r+v\kappa-\kappa)}{\eta^2(v-1)} > 0.$$

Case $*$ **II**: If $h < 0$ and $\rho = 0$, then we have the following:

$$\mathbb{U}_{1,3}^{\pm} = \pm\left[\left(\frac{i\eta(v-1)}{\sqrt{n}\kappa}\right)\left(\sqrt{\frac{ab\kappa(r+v\kappa-\kappa)}{\eta^2(v-1)}}\right)\mathrm{Sec}_{\mathrm{ab}}\left(\sqrt{\frac{\kappa(r+v\kappa-\kappa)}{\eta^2(v-1)}}(\xi)\right)\right]$$

$$e^{\left(\gamma\mathbb{W}(t)+i(vx+\kappa t+\varphi)-\frac{\gamma^2 t}{2}\right)},$$

$$Q_{1,3}^{\pm} = \pm\frac{1}{m}\left[-\eta_1 + 2\eta n\left(\frac{i\eta(v-1)}{\sqrt{n}\kappa}\right)^2\left(\sqrt{\frac{ab\kappa(r+v\kappa-\kappa)}{\eta^2(v-1)}}\right)^2\mathrm{Sec}_{\mathrm{ab}}\left(\sqrt{\frac{\kappa(r+v\kappa-\kappa)}{\eta^2(v-1)}}(\xi)\right)^2\right],$$

$$\mathbb{U}_{1,4} = \pm\left[\left(\frac{i\eta(v-1)}{\sqrt{n}\kappa}\right)\left(\sqrt{\frac{ab\kappa(r+v\kappa-\kappa)}{\eta^2(v-1)}}\right)\mathrm{Csc}_{\mathrm{ab}}\left(\sqrt{\frac{\kappa(r+v\kappa-\kappa)}{\eta^2(v-1)}}(\xi)\right)\right]$$

$$e^{\left(\gamma\mathbb{W}(t)+i(vx+\kappa t+\varphi)-\frac{\gamma^2 t}{2}\right)},$$

$$Q_{1,4}^{\pm} = \pm\frac{1}{m}\left[-\eta_1 + 2\eta n\left(\frac{i\eta(v-1)}{\sqrt{n}\kappa}\right)^2\left(\sqrt{\frac{ab\kappa(r+v\kappa-\kappa)}{\eta^2(v-1)}}\right)^2\mathrm{Csc}_{\mathrm{ab}}\left(\sqrt{\frac{\kappa(r+v\kappa-\kappa)}{\eta^2(v-1)}}(\xi)\right)^2\right],$$

where

$$\xi = \eta t + sx, \qquad \frac{ab\kappa(r+v\kappa-\kappa)}{\eta^2(v-1)} > 0, \qquad and \qquad \frac{\kappa(r+v\kappa-\kappa)}{\eta^2(v-1)} > 0.$$

Case $*$ **III**: If $h < 0$ and $\rho = \frac{\delta^2}{4}$, then we have the following:

$$\mathbb{U}_{1,5}^{\pm} = \pm\left[\left(\frac{i\eta(v-1)}{\sqrt{n}\kappa}\right)\left(\sqrt{\frac{\kappa(r+v\kappa-\kappa)}{2\eta^2(v-1)}}\right)\mathrm{Tanh}_{ab}\left(\sqrt{\frac{\kappa(r+v\kappa-\kappa)}{2\eta^2(v-1)}}(\xi)\right)\right]e^{\left(\gamma\mathbb{W}(t)+i(vx+\kappa t+\varphi)-\frac{\gamma^2 t}{2}\right)},$$

$$Q_{1,5}^{\pm} = \pm\frac{1}{m}\left[-\eta_1 + 2\eta n\left(\frac{i\eta(v-1)}{\sqrt{n}\kappa}\right)^2\left(\sqrt{\frac{\kappa(r+v\kappa-\kappa)}{2\eta^2(v-1)}}\right)^2 \mathrm{Tanh}_{ab}\left(\sqrt{\frac{\kappa(r+v\kappa-\kappa)}{2\eta^2(v-1)}}(\xi)\right)^2\right],$$

$$\mathbb{U}_{1,6}^{\pm} = \pm\left[\left(\frac{i\eta(v-1)}{\sqrt{n}\kappa}\right)\left(\sqrt{\frac{\kappa(r+v\kappa-\kappa)}{2\eta^2(v-1)}}\right)\mathrm{Coth}_{ab}\left(\sqrt{\frac{\kappa(r+v\kappa-\kappa)}{2\eta^2(v-1)}}(\xi)\right)\right]e^{\left(\gamma\mathbb{W}(t)+i(vx+\kappa t+\varphi)-\frac{\gamma^2 t}{2}\right)},$$

$$Q_{1,6}^{\pm} = \pm\frac{1}{m}\left[-\eta_1 + 2\eta n\left(\frac{i\eta(v-1)}{\sqrt{n}\kappa}\right)^2\left(\sqrt{\frac{\kappa(r+v\kappa-\kappa)}{2\eta^2(v-1)}}\right)^2 \mathrm{Coth}_{ab}\left(\sqrt{\frac{\kappa(r+v\kappa-\kappa)}{2\eta^2(v-1)}}(\xi)\right)^2\right],$$

$$\mathbb{U}_{1,7}^{\pm} = \pm[\left(\frac{i\eta(v-1)}{\sqrt{n}\kappa}\right)(\frac{\sqrt{\frac{\kappa(r+v\kappa-\kappa)}{\eta^2(v-1)}}}{\sqrt{2}}(\mathrm{Tanh}_{ab}\left(\sqrt{2\frac{\kappa(r+v\kappa-\kappa)}{\eta^2(v-1)}}(\xi)\right) \pm i\sqrt{ab}$$

$$\mathrm{Sech}_{ab}\left(\sqrt{2\frac{\kappa(r+v\kappa-\kappa)}{\eta^2(v-1)}}(\xi)\right)))]e^{\left(\gamma\mathbb{W}(t)+i(vx+\kappa t+\varphi)-\frac{\gamma^2 t}{2}\right)},$$

$$Q_{1,7}^{\pm} = \pm\frac{1}{m}[-\eta_1 + 2\eta n\left(\frac{i\eta(v-1)}{\sqrt{n}\kappa}\right)^2(\sqrt{\frac{\kappa(r+v\kappa-\kappa)}{2\eta^2(v-1)}}(\mathrm{Tanh}_{ab}\left(\sqrt{2\frac{\kappa(r+v\kappa-\kappa)}{\eta^2(v-1)}}(\xi)\right) \pm i\sqrt{ab}$$

$$\mathrm{Sech}_{ab}\left(\sqrt{2\frac{\kappa(r+v\kappa-\kappa)}{\eta^2(v-1)}}(\xi)\right))^2],$$

$$\mathbb{U}_{1,8}^{\pm} = \pm[\frac{i\eta(v-1)}{\sqrt{n}\kappa}(\frac{\sqrt{\frac{\kappa(r+v\kappa-\kappa)}{\eta^2(v-1)}}}{\sqrt{2}}(\mathrm{Coth}_{ab}\left(\sqrt{2\frac{\kappa(r+v\kappa-\kappa)}{\eta^2(v-1)}}(\xi)\right) \pm \sqrt{ab}$$

$$\mathrm{Csch}_{ab}\left(\sqrt{2\frac{\kappa(r+v\kappa-\kappa)}{\eta^2(v-1)}}(\xi)\right)))]e^{\left(\gamma\mathbb{W}(t)+i(vx+\kappa t+\varphi)-\frac{\gamma^2 t}{2}\right)},$$

$$Q_{1,8}^{\pm} = \pm\frac{1}{m}[-\eta_1 + 2\eta n\left(\frac{i\eta(v-1)}{\sqrt{n}\kappa}\right)^2(\sqrt{\frac{\kappa(r+v\kappa-\kappa)}{2\eta^2(v-1)}}(\mathrm{Coth}_{ab}\left(\sqrt{2\frac{\kappa(r+v\kappa-\kappa)}{\eta^2(v-1)}}(\xi)\right) \pm$$

$$\sqrt{ab}\mathrm{Csch}_{ab}\left(\sqrt{2\frac{\kappa(r+v\kappa-\kappa)}{\eta^2(v-1)}}(\xi)\right))^2],$$

$$\mathbb{U}_{1,9}^{\pm} = \pm\left[\frac{i\eta(v-1)}{\sqrt{n}\,\kappa}\left(\pm\frac{\sqrt{\frac{\kappa\,(r+v\kappa-\kappa)}{\eta^2(v-1)}}}{2\sqrt{2}}\right)\left(\coth_{ab}\left(\frac{\sqrt{\frac{\kappa\,(r+v\kappa-\kappa)}{\eta^2(v-1)}}\,\xi}{2\sqrt{2}}\right)+\right.\right.$$

$$\left.\left.\times\tanh_{ab}\left(\frac{\sqrt{\frac{\kappa\,(r+v\kappa-\kappa)}{\eta^2(v-1)}}\,\xi}{2\sqrt{2}}\right)\right)\right]e^{\left(\gamma\mathbb{W}(t)+i\left(vx+\kappa t+\varphi\right)-\frac{\gamma^2 t}{2}\right)}.$$

$$Q^{\pm}_{1,9} = \pm\frac{1}{m}[-\eta_1 + 2\eta n\left(\frac{i\eta(v-1)}{\sqrt{n}\kappa}\right)^2 (\frac{\sqrt{\frac{\kappa(r+v\kappa-\kappa)}{\eta^2(v-1)}}}{2\sqrt{2}}(\mathrm{Coth}_{ab}\left(\frac{\sqrt{\frac{\kappa(r+v\kappa-\kappa)}{\eta^2(v-1)}}(\xi)}{2\sqrt{2}}\right)+$$

$$\mathrm{Tanh}_{ab}\left(\frac{\sqrt{\frac{\kappa(r+v\kappa-\kappa)}{\eta^2(v-1)}}(\xi)}{2\sqrt{2}}\right))^2],$$

where

$$\xi = \eta t + sx, \quad \text{and} \quad \frac{\kappa(r+v\kappa-\kappa)}{\eta^2(v-1)} > 0.$$

Case $*$ **IV**: If $h > 0$ and $\rho = \frac{h^2}{4}$, then we have the following:

$$\mathbb{U}^{\pm}_{1,10} = \pm\left[\left(\frac{i\eta(v-1)}{\sqrt{n}\kappa}\right)\left(\sqrt{-\frac{\kappa(r+v\kappa-\kappa)}{2\eta^2(v-1)}}\right)\mathrm{Tan}_{ab}\left(\sqrt{-\frac{\kappa(r+v\kappa-\kappa)}{2\eta^2(v-1)}}(\xi)\right)\right]e^{\left(\gamma\mathbb{W}(t)+i(vx+\kappa t+\varphi)-\frac{\gamma^2 t}{2}\right)},$$

$$Q^{\pm}_{1,10} = \pm\frac{1}{m}\left[-\eta_1 + 2\eta n\left(\frac{i\eta(v-1)}{\sqrt{n}\kappa}\right)^2\left(\sqrt{-\frac{\kappa(r+v\kappa-\kappa)}{2\eta^2(v-1)}}\right)^2\mathrm{Tan}_{ab}\left(\sqrt{-\frac{\kappa(r+v\kappa-\kappa)}{2\eta^2(v-1)}}(\xi)\right)^2\right],$$

$$\mathbb{U}^{\pm}_{1,11} = \pm\left[\left(\frac{i\eta(v-1)}{\sqrt{n}\kappa}\right)\left(\sqrt{-\frac{\kappa(r+v\kappa-\kappa)}{2\eta^2(v-1)}}\right)\mathrm{Cot}_{ab}\left(\sqrt{-\frac{\kappa(r+v\kappa-\kappa)}{2\eta^2(v-1)}}(\xi)\right)\right]e^{\left(\gamma\mathbb{W}(t)+i(vx+\kappa t+\varphi)-\frac{\gamma^2 t}{2}\right)},$$

$$Q^{\pm}_{1,11} = \pm\frac{1}{m}\left[-\eta_1 + 2\eta n\left(\frac{i\eta(v-1)}{\sqrt{n}\kappa}\right)^2\left(\sqrt{-\frac{\kappa(r+v\kappa-\kappa)}{2\eta^2(v-1)}}\right)^2\mathrm{Cot}_{ab}\left(\sqrt{-\frac{\kappa(r+v\kappa-\kappa)}{2\eta^2(v-1)}}(\xi)\right)^2\right],$$

$$\mathbb{U}^{\pm}_{1,12} = \pm\left[\left(\frac{i\eta(v-1)}{\sqrt{n}\kappa}\right)\left(\sqrt{-\frac{\kappa(r+v\kappa-\kappa)}{2\eta^2(v-1)}}\times\left(\mathrm{Tan}_{ab}\left(\sqrt{-2\frac{\kappa(r+v\kappa-\kappa)}{\eta^2(v-1)}}\,\xi\right)\pm\sqrt{ab}\right.\right.\right.$$

$$\left.\left.\left.\mathrm{Sec}_{ab}\left(\sqrt{-2\frac{\kappa(r+v\kappa-\kappa)}{\eta^2(v-1)}}\,\xi\right)\right)\right)\right]\times e^{\left(\gamma\mathbb{W}(t)+i(vx+\kappa t+\varphi)-\frac{\gamma^2 t}{2}\right)}$$

$$Q^{\pm}_{1,12} = \pm\frac{1}{m}\left[-\eta_1 + 2\eta n\left(\frac{i\eta(v-1)}{\sqrt{n}\kappa}\right)^2\left(\sqrt{-\frac{\kappa(r+v\kappa-\kappa)}{2\eta^2(v-1)}}\left(\mathrm{Tan}_{ab}\left(\sqrt{-2\frac{\kappa(r+v\kappa-\kappa)}{\eta^2(v-1)}}(\xi)\right)\pm\sqrt{ab}\right.\right.\right.\right.$$

$$\left.\left.\left.\left.\times\,\mathrm{Sec}_{ab}\left(\sqrt{-2\frac{\kappa(r+v\kappa-\kappa)}{\eta^2(v-1)}}(\xi)\right)\right)\right)^2\right],$$

$$\mathbb{U}^{\pm}_{1,13} = \pm\left[\left(\frac{i\eta(v-1)}{\sqrt{n}\kappa}\right)\left(\sqrt{-\frac{\kappa(r+v\kappa-\kappa)}{2\eta^2(v-1)}}\left(\mathrm{Cot}_{ab}\left(\sqrt{-2\frac{\kappa(r+v\kappa-\kappa)}{\eta^2(v-1)}}(\xi)\right)\pm\right.\right.\right.$$

$$\left.\left.\left.\times\,\sqrt{ab}\mathrm{Csc}_{ab}\left(\sqrt{-2\frac{\kappa(r+v\kappa-\kappa)}{\eta^2(v-1)}}(\xi)\right)\right)\right)\right]e^{\left(\gamma\mathbb{W}(t)+i(vx+\kappa t+\varphi)-\frac{\gamma^2 t}{2}\right)},$$

$$Q^{\pm}_{1,13} = \pm\frac{1}{m}\Bigg[-\eta_1 + 2\eta n\left(\frac{i\eta(v-1)}{\sqrt{n}\kappa}\right)^2\left(\sqrt{-\frac{\kappa(r+v\kappa-\kappa)}{2\eta^2(v-1)}}\left(\mathrm{Cot}_{ab}\left(\sqrt{-2\frac{\kappa(r+v\kappa-\kappa)}{\eta^2(v-1)}}(\xi)\right)\pm\sqrt{ab}\right.\right.$$
$$\left.\left.\times\,\mathrm{Csc}_{ab}\left(\sqrt{-2\frac{\kappa(r+v\kappa-\kappa)}{\eta^2(v-1)}}(\xi)\right)\right)\right)^2\Bigg],$$

$$\mathbb{U}^{\pm}_{1,14} = \pm\Bigg[\left(\frac{i\eta(v-1)}{\sqrt{n}\kappa}\right)\left(\frac{\sqrt{-\frac{\kappa(r+v\kappa-\kappa)}{\eta^2(v-1)}}}{2\sqrt{2}}\left(\mathrm{Cot}_{ab}\left(\frac{\sqrt{-\frac{\kappa(r+v\kappa-\kappa)}{\eta^2(v-1)}}(\xi)}{2\sqrt{2}}\right)+\right.\right.$$
$$\left.\left.\times\,\mathrm{Tan}_{ab}\left(\frac{\sqrt{-\frac{\kappa(r+v\kappa-\kappa)}{\eta^2(v-1)}}(\xi)}{2\sqrt{2}}\right)\right)\right]e^{\left(\gamma\bar{W}(t)+i(vx+\kappa t+\varphi)-\frac{\gamma^2 t}{2}\right)},$$

$$Q^{\pm}_{1,14} = \pm\frac{1}{m}\Bigg[-\eta_1 + 2\eta n\left(\frac{i\eta(v-1)}{\sqrt{n}\kappa}\right)^2\left(\frac{\sqrt{-\frac{\kappa(r+v\kappa-\kappa)}{\eta^2(v-1)}}}{2\sqrt{2}}\left(\mathrm{Cot}_{ab}\left(\frac{\sqrt{-\frac{\kappa(r+v\kappa-\kappa)}{\eta^2(v-1)}}(\xi)}{2\sqrt{2}}\right)+\right.\right.$$
$$\left.\left.\times\,\mathrm{Tan}_{ab}\left(\frac{\sqrt{-\frac{\kappa(r+v\kappa-\kappa)}{\eta^2(v-1)}}(\xi)}{2\sqrt{2}}\right)\right)\right)^2\Bigg],$$

where

$$\xi = \eta t + sx, \quad \textit{and} \quad -\frac{\kappa(r+v\kappa-\kappa)}{\eta^2(v-1)} > 0.$$

4. Simulation and discussion

The 3D solution graphs denote the time progress of the solitons with a smoother and definite propagation centered on time. These results confirm the correctness of the analytical solutions and highlight the stability of the soliton profiles in the absence of perturbations. In contrast, the stochastic 3D graphs demonstrate how random fluctuations influence the dynamical behavior of the system. Specifically, the oscillations of the soliton amplitude and the width in response to stochastic noise indicate how sensitive the system is to external noise and irregularities in dispersion. These effects provide a physical interpretation of the modeled dynamics, showing that the obtained solutions remain valid under uncertainties. Additionally, the stability properties and bifurcation trends are further accentuated in the solution and analysis graphs, which further reinforce the relationship between the analytical solution and its physical implications.

To evaluate the physical reliability of these solutions, we utilized a Monte Carlo approach that involved the ensemble averaging of $N = 20$ independent stochastic realizations. Rather than relying on a single snapshot, this statistical method allows us to observe how the waves behave in a realistic, noisy environment. The Ensemble Mean Profiles (Figures 1–12) demonstrate remarkable structural stability. Despite the presence of Brownian noise, the bright and dark soliton morphologies remain intact. This suggests that the nonlinearity in the CKM effectively acts as a self-correcting force that prevents the wave from dissipating. Our Variance and Standard Deviation maps (Figures 1–12) further reveal that

the fluctuations are not randomly spread but are localized at the high-energy wave crests. Physically, this anchoring is crucial for applications such as optical fiber communication, as it implies that while noise may cause a minor amplitude jitter, the signal's core coherence is preserved over long distances. Similarly, in biological microtubules, this clustering ensures that ionic signals remain distinct despite microscopic thermal chatter. The 2D Ensemble plots (Figures 1–12) confirm this by showing individual random paths (gray lines) tightly clustered around the mean trajectory. This proves that our solutions are not mere mathematical artifacts but are robust enough to sustain information transport in the open (noisy) systems common in experimental physics and biology.

The noise intensity parameter γ is a very important factor in determining the stochastic process of the derived solitary wave solutions. When $\gamma = 0$, the system reverts to its deterministic form, and the soliton waves propagate with a constant amplitude and wave shape, as observed in the smooth mean wave profiles in (Figures 1–12). With an increasing γ, the Wiener process adds a multiplicative white noise component that gives rise to amplitude fluctuations and surface roughening, which are most evident at the wave peaks because of the multiplicative nature of the noise term $\gamma\frac{dW(t)}{dt}U$. However, the soliton wave shape is retained, as evidenced by the strong clustering of the 20 Monte Carlo simulations around the ensemble mean in the 2D plots (panel e) in all figures. This clearly shows that the nonlinear and dispersive components of the Kuralay model provide a self-correcting process that ensures the derived solutions are physically valid and meaningful even in the presence of stochastic noise perturbations.

Without white noise, the solitons behave predictably, whereas the introduction of white noise leads changes in their trajectories, shapes, amplitudes, and velocities. White noise influence solitons are crucial for applications in nonlinear optics, telecommunications, and plasma physics [30,31], providing insights into managing noise in complex systems. Here, we show 3D and 2D visualizations of the obtained solutions.

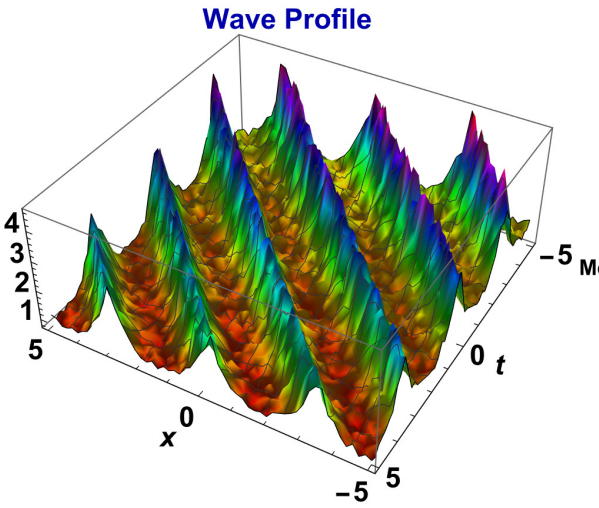

(a) 3D Stochastic Solitary Wave Profile

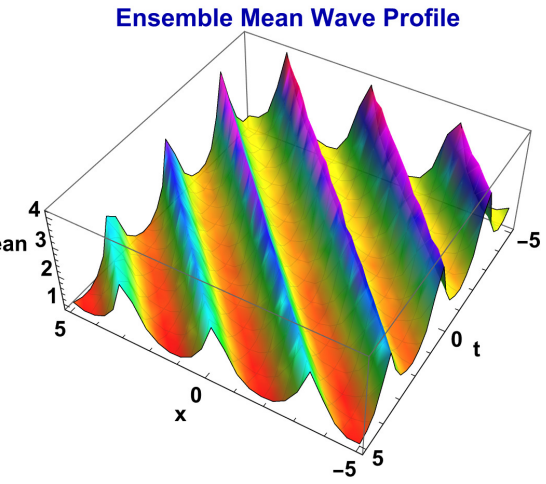

(b) 3D Mean Solitary Wave

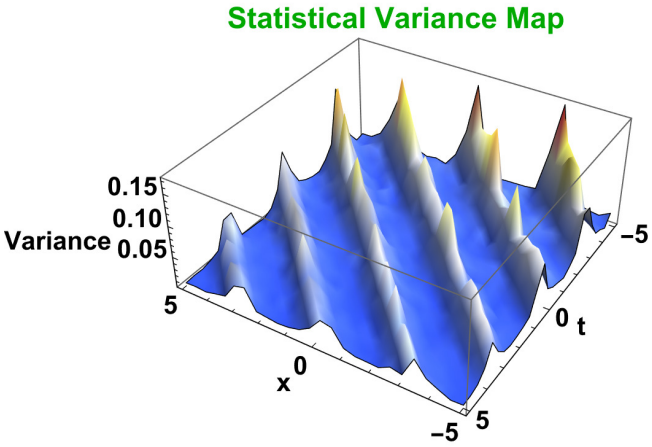

(c) 3D Variance Solitary Wave

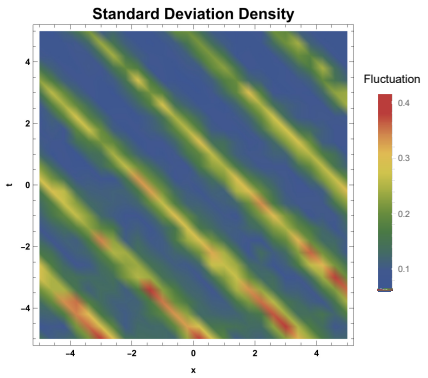

(d) Standard Deviation of Stochastic Solitary Wave

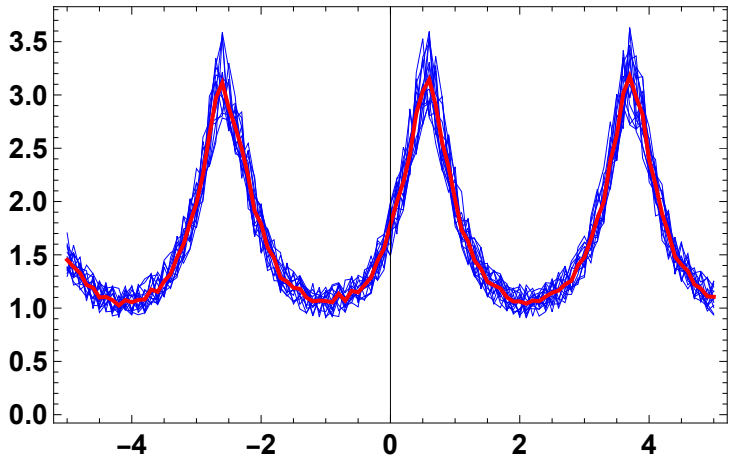

(e) 2D Ensemble Average Vs Mean

Figure 1. Parameters used for the above 3D and 2D plots of $|\mathbb{U}^{+}_{1,1}|$ are $a = 0.5$, $b = \nu = \kappa = \wp = e = r = 1$, and $\eta = i$, while keeping the intensity $\gamma = 1$, with $\nu = 2$.

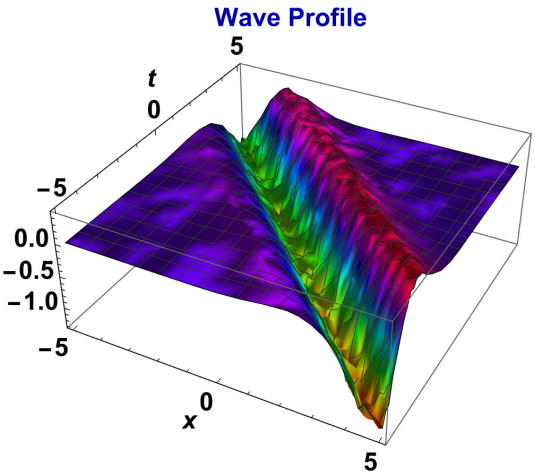

(a) 3D Stochastic Solitary Wave Profile

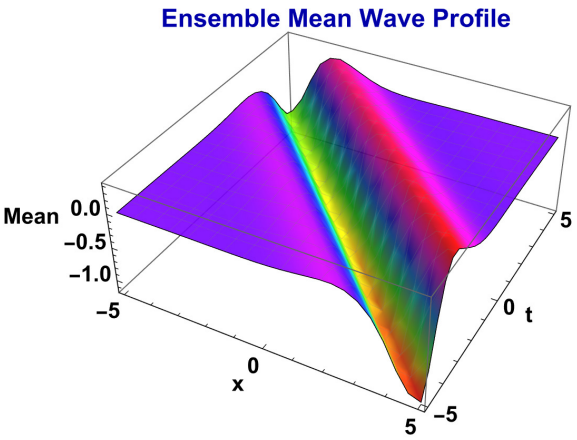

(b) 3D Mean of Stochatic Solitary Wave

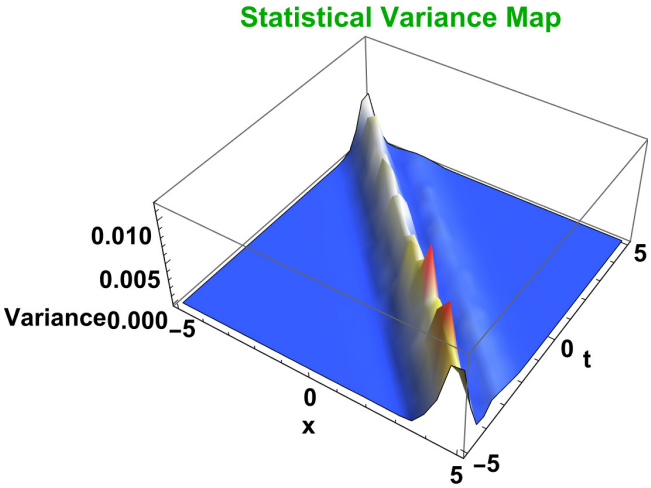

(c) 3D Variance of Stochastic Solitary Wave

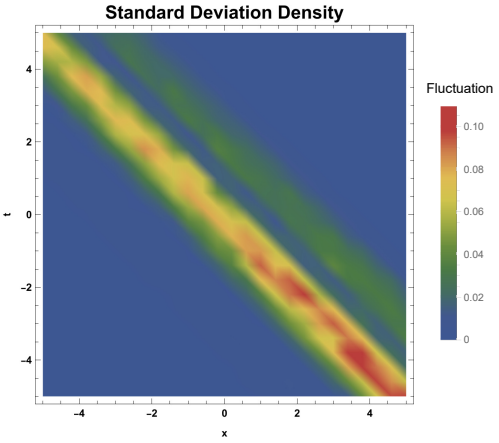

(d) Standard Deviation of Stochastic Solitary Wave

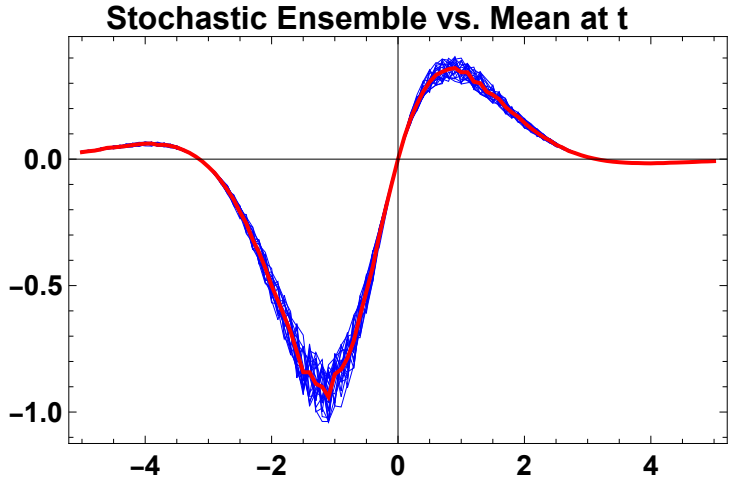

(e) 2D Ensemble average Vs Mean Stochastic Solitary Wave

Figure 2. Parameters used for the above 3D and contour plots of $Re(\mathbb{U}^{+}_{1,1})$ are $a = 0.5$, $b = \nu = \kappa = \wp = e = r = 1$, and $\eta = i$, while the intensity $\gamma = 1$, $\nu = 2$.

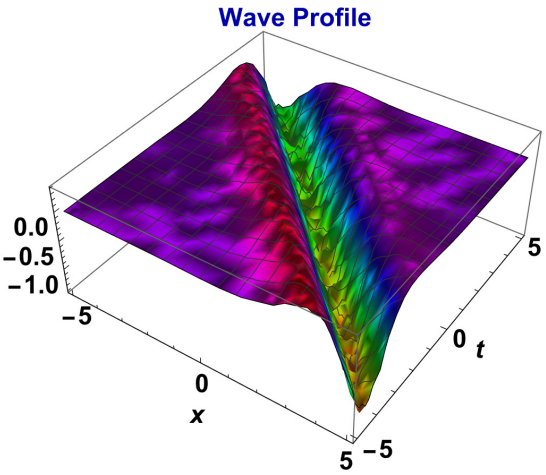

(a) 3D Stochastic Solitary Wave

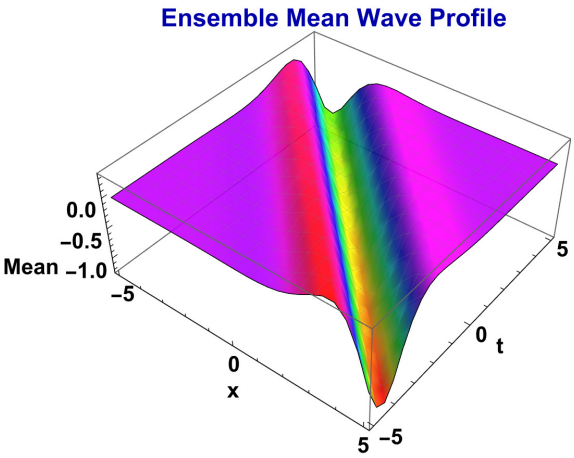

(b) 3D Mean of Stochastic Solitary Wave

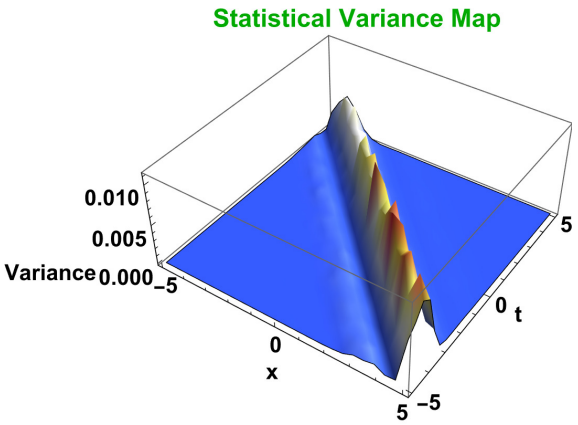

(c) 3D Variance of Stochastic Solitary Wave

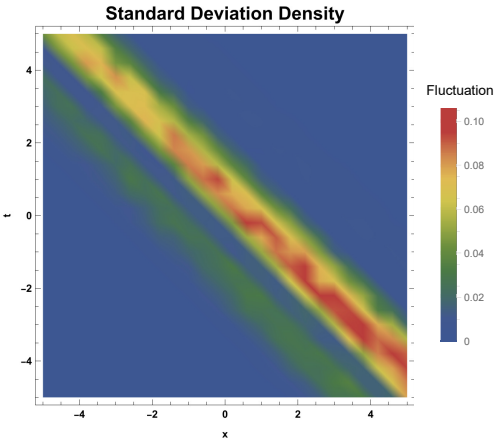

(d) Standard Deviation of Stochastic Solitary Wave

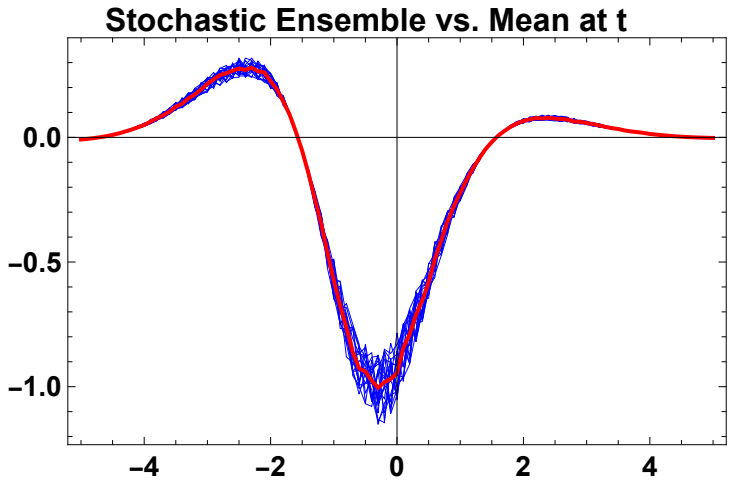

(e) 2D Ensemble Average Vs Mean of Stochastic Solitary Wave

Figure 3. Parameters used for the above 3D and contour plots of $Im(\mathbb{U}^{+}_{1,1})$ are $a = 0.5$, $b = \nu = \kappa = \wp = e = r = 1, \eta = i$, and $\nu = 2$, and the intensity $\gamma = 1$.

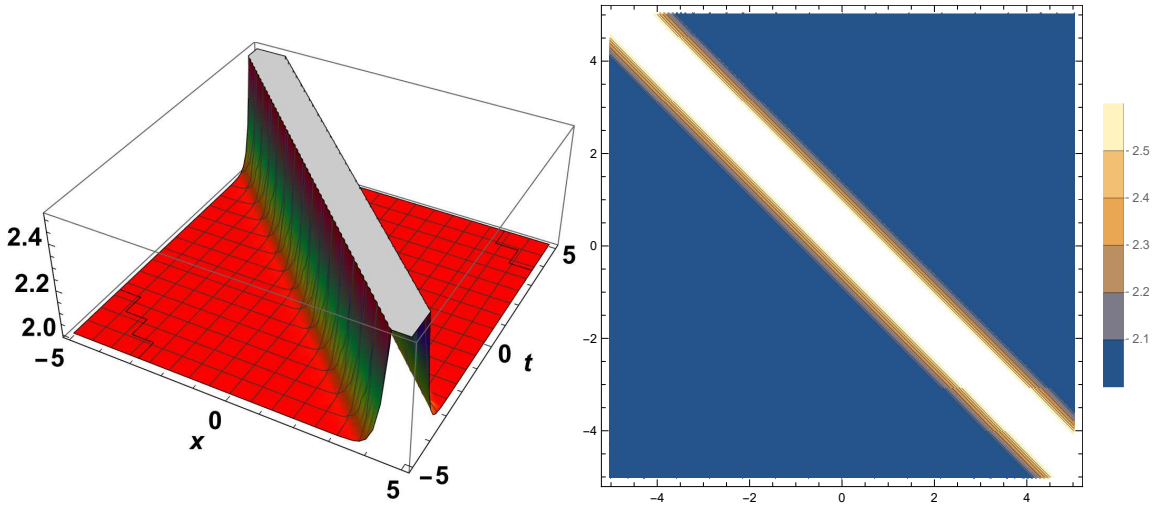

(a) 3D Solitary Wave Profile **(b)** 3D Stochastic Solitary Wave

Figure 4. Here, the parameters used for the 3D and contour plots of $Q_{1,1}$ are $a = 0.5$, $b = \nu = \kappa = \wp = e = r = 1, \eta = i, \eta 1 = 2$, and $v = 2$.

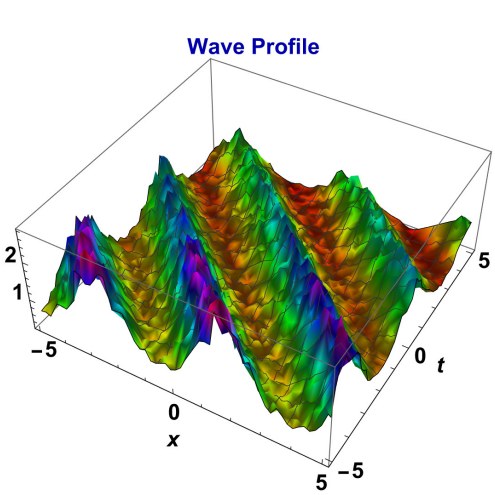

(a) 3D Stochastic Solitary Wave

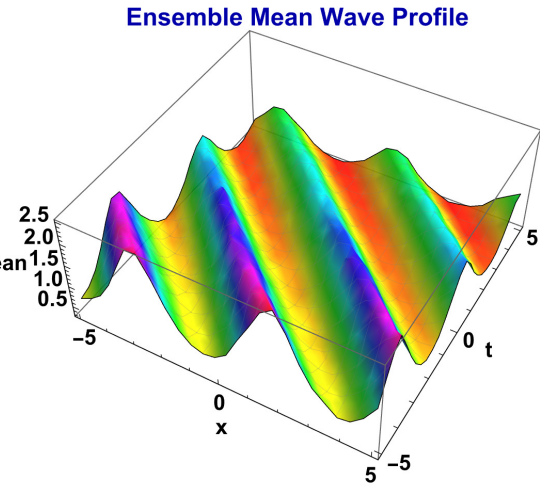

(b) 3D Mean of Stochastic Solitary Wave

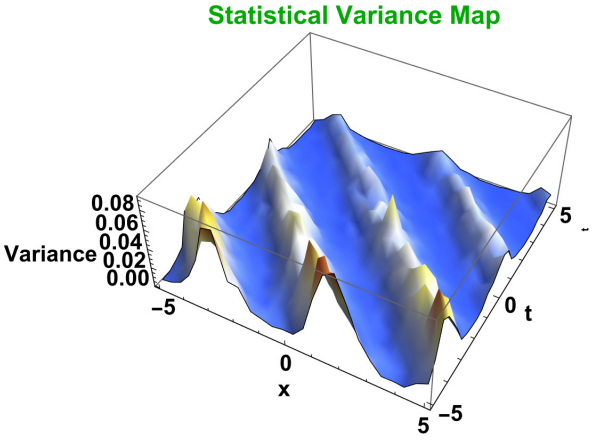

(c) 3D Variance of Stochastic Solitary Wave

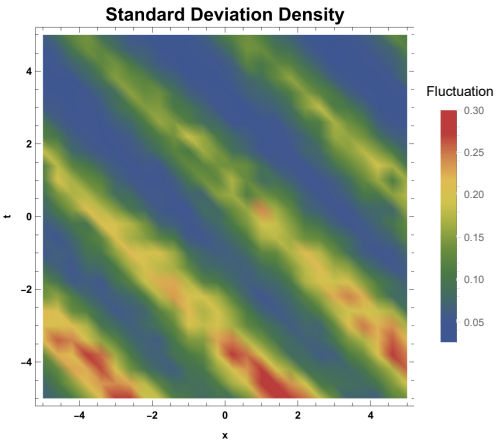

(d) Standard Deviation of Stochastic Solitary Wave

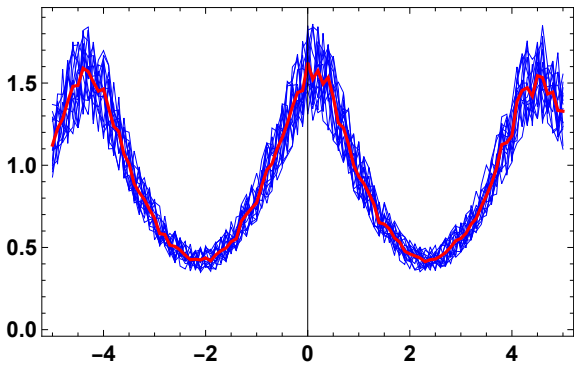

(e) 2D Ensemble Average Vs Mean of Solitary Wave

Figure 5. Here, the parameters used for the 3D and 2D plots of $|\mathbb{U}^{+}_{1,7}|$ are $a = 0.1$, $\nu = b = \kappa = \wp = \eta = e = 1$, $r = -2$, and $v = 2$, while keeping the intensity $\gamma = 1$.

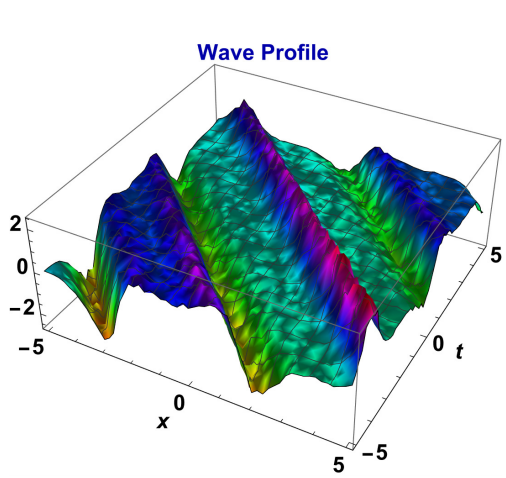

(a) 3D Stochastic Solitary Wave

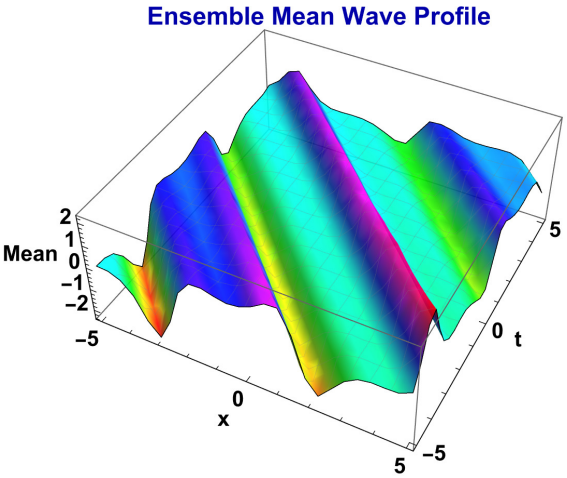

(b) 3D Mean of Stochastic Solitary Wave

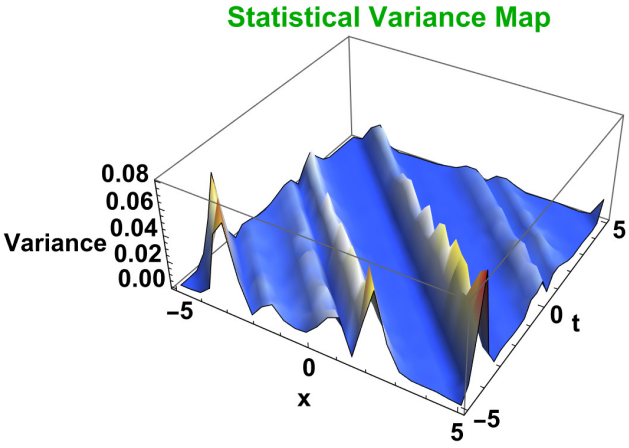

(c) 3D Variance of Stochastic Solitary Wave

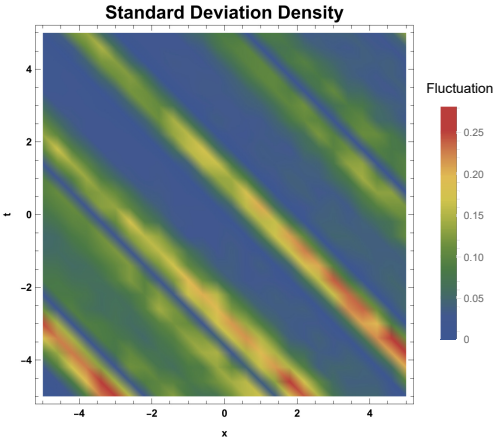

(d) Standard Deviation of Stochastic Solitary Wave

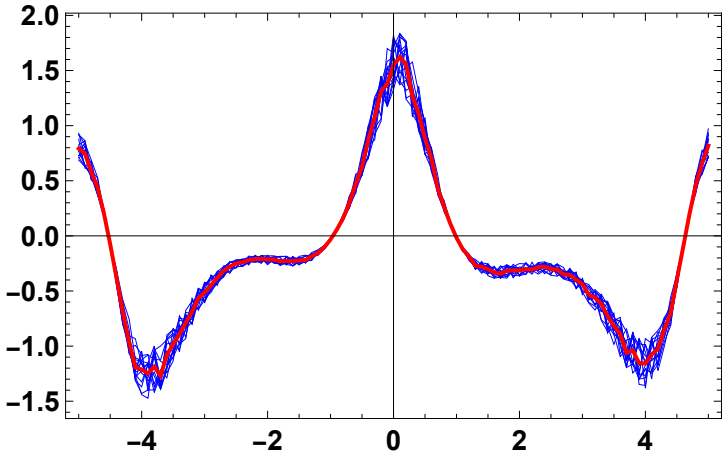

(e) 2D Ensemble Average Vs Mean of Stochastic Solitary Wave

Figure 6. Here, the parameters used for the 3D and 2D plots of $Re(\mathbb{U}^{+}_{1,7})$ are $a = 0.1$, $\nu = b = \kappa = \wp = \eta = e = 1$, $r = -2$, and $v = 2$, while keeping the intensity $\gamma = 1$.

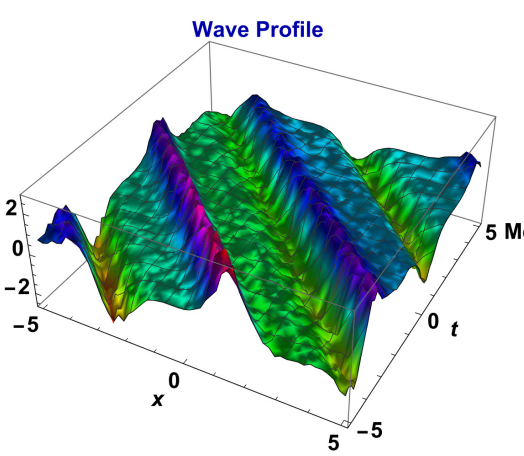

(a) 3D Stochastic Solitary Wave

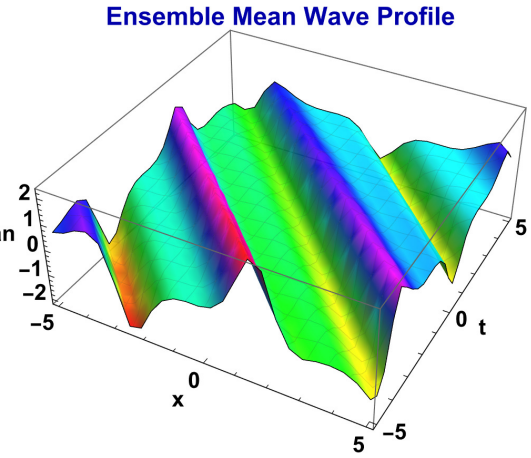

(b) 3D Mean of Stochastic Solitary Wave

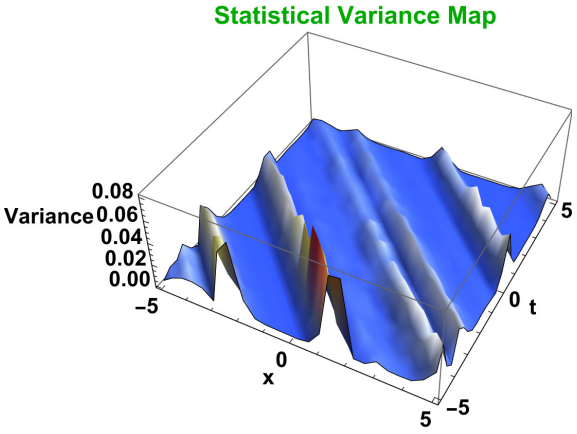

(c) 3D Variance of Stochastic Solitary Wave

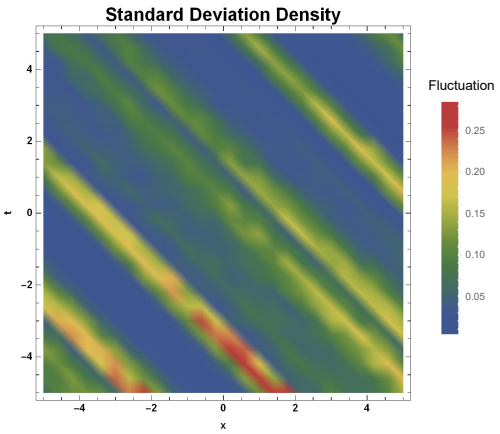

(d) Standard Deviation of Stochastic Solitary Wave

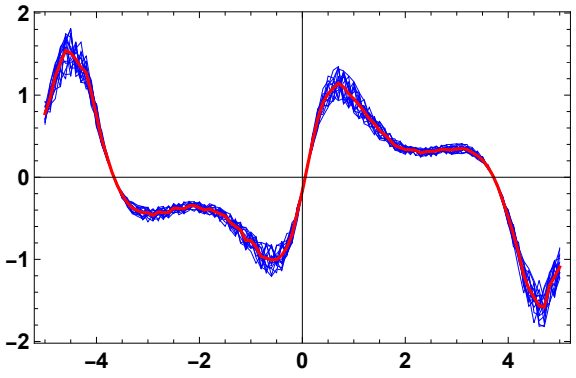

(e) 2D Stochastic Ensemble Vs Mean at $t = 1$

Figure 7. Here, the parameters used for the 3D and contour plots of $Im(\mathbb{U}^{+}_{1,7})$ are $a = 0.1,\ \nu = b = \kappa = \wp = \eta = e = 1,\ r = -2,$ and $v = 2$, while keeping the intensity $\gamma = 1$.

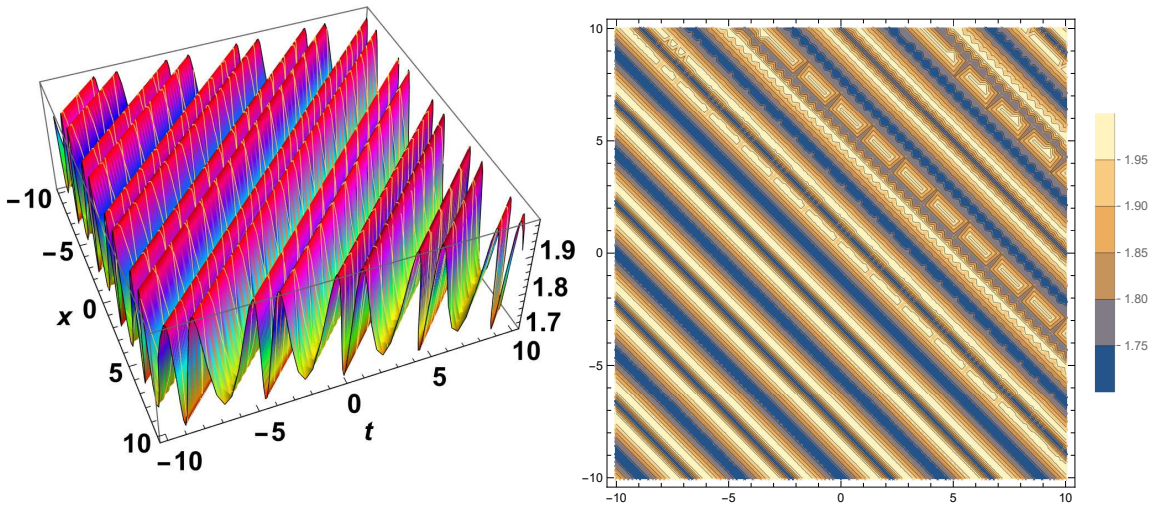

(a) 3D Solitary Wave **(b)** Contour Solitary Wave

Figure 8. Here, the parameters used for the 3D and contour plots of $Q_{1,7}$ are $a = 0.1,\ \nu = b = \kappa = \wp = \eta = e = 1,\ \eta 1 = 2,\ r = -2,$ and $v = 2$.

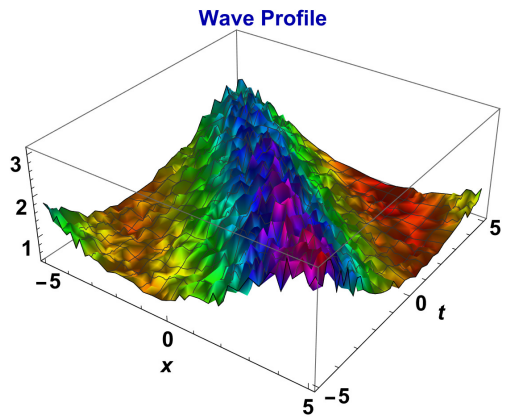

(a) 3D Solitary Wave

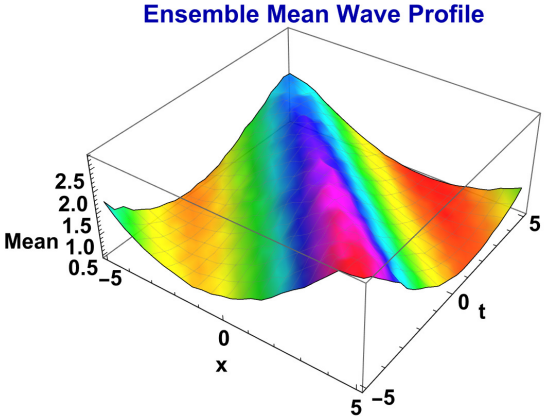

(b) 3D Mean of Stochastic Solitary Wave

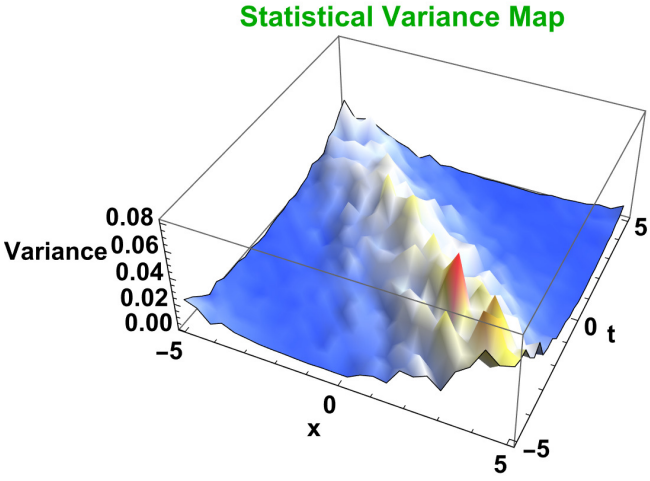

(c) 3D Variance of Stochastic Solitary Wave

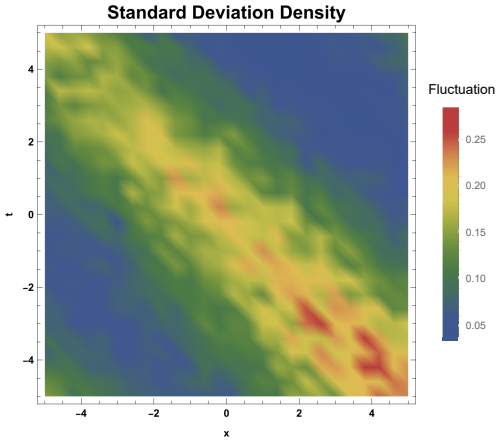

(d) Standard Deviation of Stochastic Solitary Wave

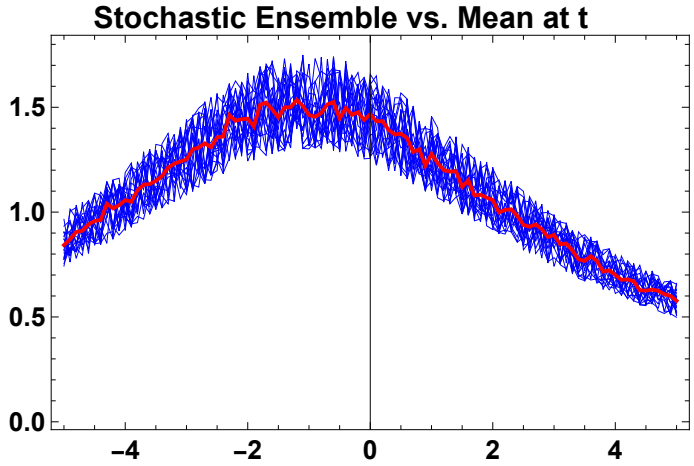

(e) 2D Stochastic Ensemble Vs Mean at time $t = 1$

Figure 9. In the figure above, we used the following parameters to plot the 3D and 2D graphs for $|\mathbb{U}^{+}_{1,13}|$: $a = 0.1$, $\nu = b = \kappa = \wp = e = r = 1$, $v = 2$, and $\eta = i$, while setting the intensity $\gamma = 1$.

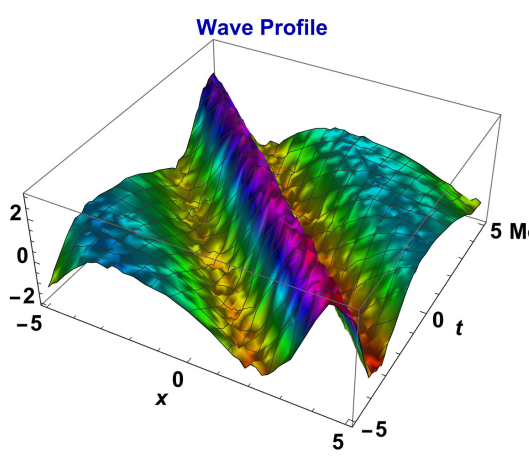

(a) 3D Stochastic Solitary Wave

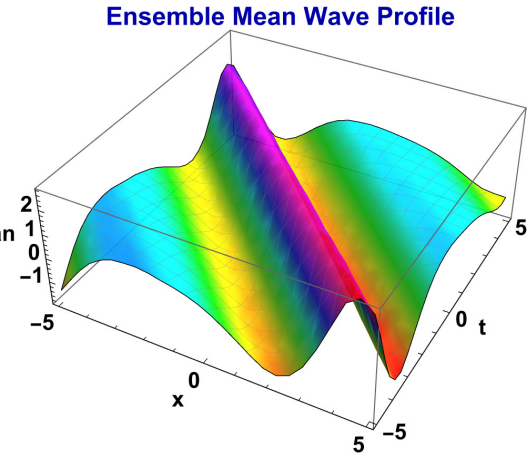

(b) 3D Mean of Stochastic Solitary Wave

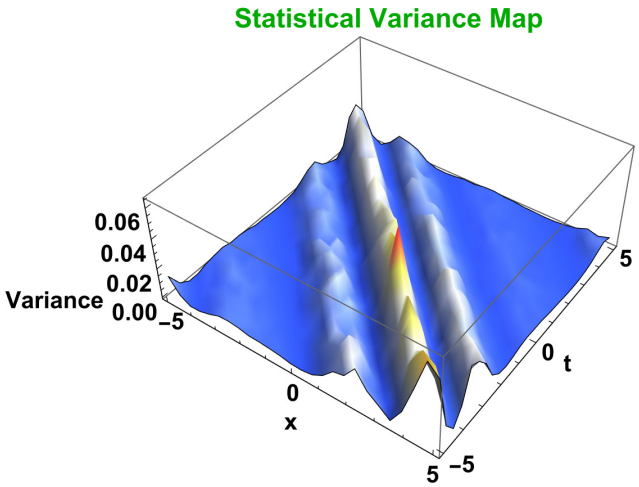

(c) 3D Variance of Stochastic Solitary Wave

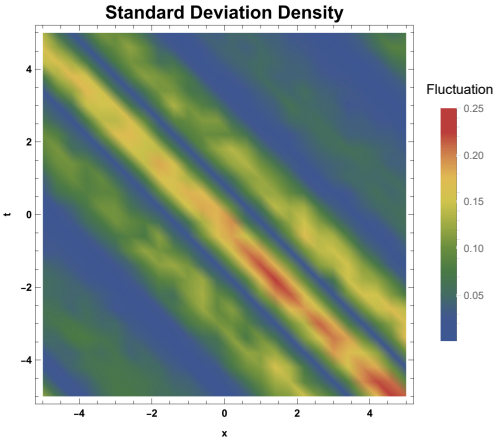

(d) Standard Deviation of Stochastic Solitary Wave

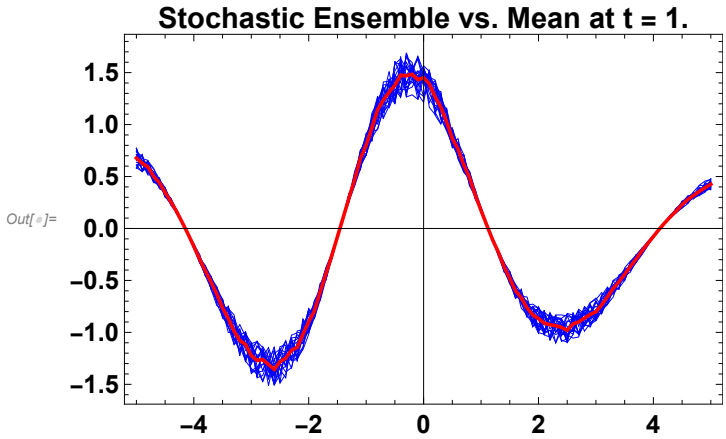

(e) 2D Stochastic Ensemble Vs Mean at time $t = 1$

Figure 10. In the figure above, we used the following parameters to plot the 3D and 2D graphs for $Re(\mathbb{U}^{+}_{1,13})$: $a = 0.1$, $\nu = b = \kappa = \wp = e = r = 1$, $\eta = i$, and $v = 2$, with the intensity $\gamma = 1$.

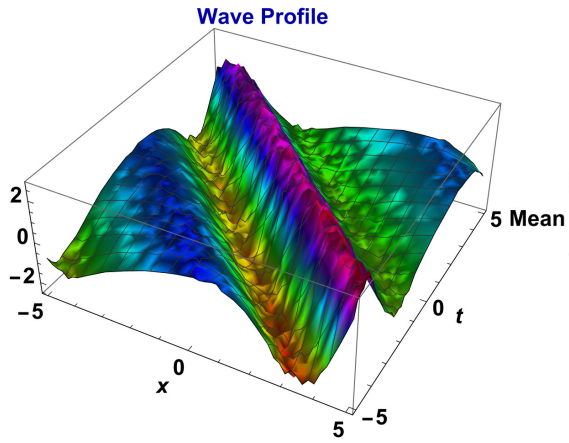

(a) 3D Stochastic Solitary Wave

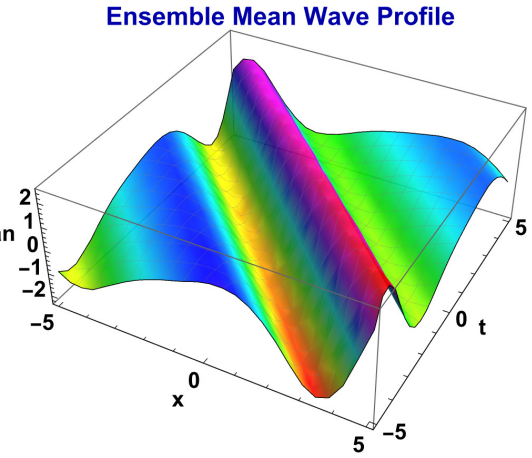

(b) 3D Mean of Stochastic Solitary Wave

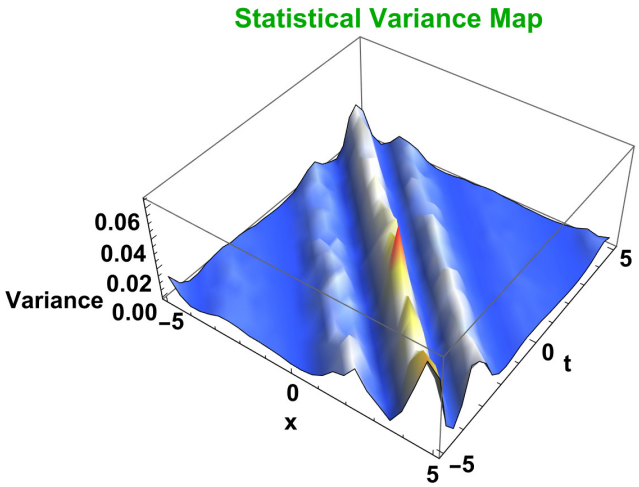

(c) 3D Variance of Stochastic Solitary Wave

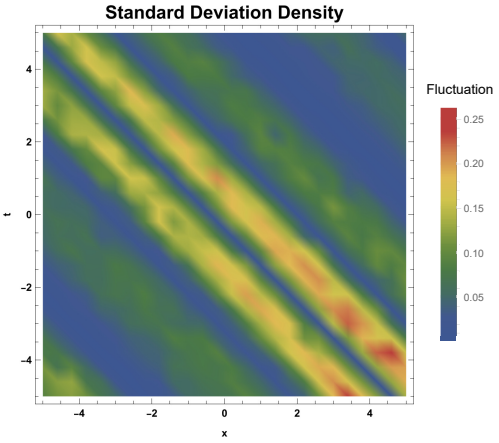

(d) Standard Deviation of Stochastic Solitary Wave

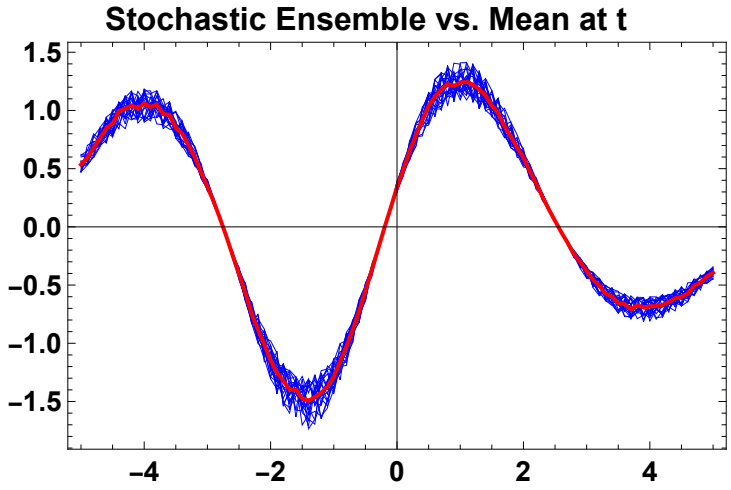

(e) 2D Stochastic Ensemble Vs Mean at time $t = 1$

Figure 11. In the figure above, we used the following parameters to plot the 3D and 2D graphs for $Re(\mathbb{U}^{+}_{1,13})$: $a = 0.1$, $\nu = b = \kappa = \wp = e = r = 1$, $\eta = i$, and $v = 2$, with the intensity $\gamma = 1$.

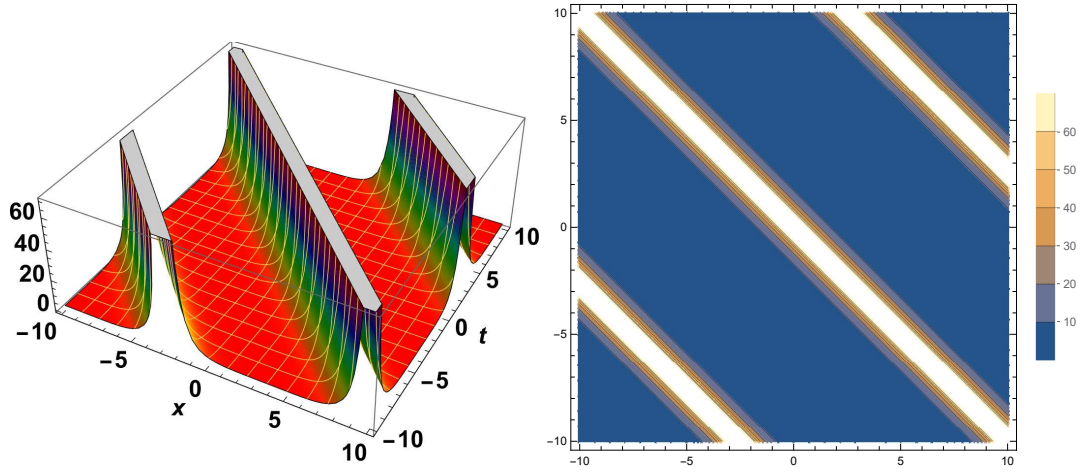

(a) 3D Solitary Wave **(b)** Contour Solitary Wave

Figure 12. Here, the parameters used for 3D and contour plots of $Q_{1,13}$ are $a = \nu = b = \kappa = \wp = \eta = e = r = 1,\ \nu = 2,$ and $\eta 1 = 2$.

5. Conclusions

This study determined the outstanding efficiency of the SSEM to solve the CCK model, thereby yielding exact soliton solutions that are essential to separate wave propagation dynamics. By joining the Wiener process, we provided a robust framework to analyze stochastic behavior, completed by 3D and contour plots that brightly captured the complex dynamics of the system. Our results exposed the stabilizing role of multiplicative noise and presented new insights into how variations influence and regulate complex systems. These results hold important implications for various fields in physics and engineering, thus providing a foundation for future investigations into nonlinear phenomena. By joining analytical accuracy with real-world complexity, this research not only advances our understanding of stochastic and nonlinear systems, but also opens new avenues to explore the interaction of noise and its consistency. Furthermore, the analysis of the noise intensity parameter γ demonstrates that although increasing the stochastic strength induces the amplitude fluctuations and surface irregularities through multiplicative Wiener perturbations, the essential soliton structure remains preserved, thus confirming the inherent stability and physical robustness of the derived solutions under stochastic effects. It is worth noting that previous studies on the complex coupled Kuralay model mainly addressed analytical solutions, whereas, in this work, we derived explicit solitary wave solutions. Furthermore, the SSEM was applied to this equation for the first time, which underscores the novelty of our approach. These contributions extend the available literature by providing new exact solutions and deeper physical insights into the system's stochastic. This comprehensive parameter exploration reveals intricate dynamical regimes, thereby highlighting the sensitivity of the system's behavior to changes in the physical parameters.In future work, we plan to extend the analysis to explore lump solutions, which represent localized wave structures with complex interactions. This work stands as a demonstration of the power of advanced mathematical approaches in decoding the mysteries of nature and engineering, paving the way for transformative findings in related domains.

6. Future directions

This study provided analytical insight into solitary wave dynamics and chaos in a stochastic CCK model using the SSEM. Several extensions of the present work can be considered in future research. One possible direction is the application of the proposed approach to higher-order and more complex stochastic nonlinear evolution equations, where additional dispersion and nonlinear effects may lead to richer wave structures. In this context, the construction of exact solutions for higher-order stochastic models, such as the modified Gerdjikov–Ivanov equation, represents a promising avenue for a further investigation [10]. Another important extension involves fractional-order stochastic models, which are capable of capturing memory and nonlocal effects in physical systems such as fluid dynamics and optical media. Analytical studies of fractional solitons in higher-dimensional nonlinear evolution equations have recently attracted significant attention and may benefit from the methodology developed in the present work [46]. Moreover, a further investigation of multiplicative noise and stochastic perturbations may enhance the understanding of the soliton stability, noise-induced chaos, and robustness of wave structures. In particular, stochastic derivative nonlinear conformable Schrödinger-type equations under multiplicative white noise and conformable derivatives by using temporal parameters provide a natural framework for such studies [34]. Adapting the proposed method to these models may lead to new exact solutions with a clear physical relevance.

Author contributions

S. Trabelsi, M. Arab: Formal analysis, investigation, supervision, project administration, funding acquisition; Beenish: Conceptualization, formal analysis, investigation; S. Yasin: Conceptualization, software, methodology, validation, visualization, formal analysis, formatting, investigation, writing—original draft, writing—review and editing. All authors have read and approved the final version of the manuscript for publication.

Use of Generative-AI tools declaration

The authors declare that no Generative-AI tools were used in the creation of this article.

Acknowledgments

The authors would like to thank the Deanship of Scientific Research, Vice Presidency for Graduate Studies and Scientific Research, King Faisal University, Saudi Arabia (Grant No. KFU261146) for their financial support, as well as the reviewers for their valuable comments.

Conflict of interest

The authors declare that there are no conflicts of interest regarding the publication of this paper.

References

1. A. Khan, T. Akram, A. Khan, S. Ahmad, K. Nonlaopon, Investigation of time-fractional nonlinear KdV–Burgers equation under fractional operators with nonsingular kernels, *AIMS Math.*, **8** (2023), 1251–1268. http://dx.doi.org/10.3934/math.2023063
2. E. Tadmor, A review of numerical methods for nonlinear partial differential equations, *Bull. Am. Math. Soc.*, **49** (2012), 507–554. http://dx.doi.org/10.1090/S0273-0979-2012-01379-4
3. S. Malik, M. S. Hashemi, S. Kumar, H. Rezazadeh, W. Mahmoud, M. S. Osman, Application of new Kudryashov method to various nonlinear partial differential equations, *Opt. Quant. Electron.*, **55** (2023), 8. https://doi.org/10.1007/s11082-022-04261-y
4. P. E. Farrell, A. Birkisson, S. W. Funke, Deflation techniques for finding distinct solutions of nonlinear partial differential equations, *SIAM J. Sci. Comput.*, **37** (2015), A2026–A2045. https://doi.org/10.48550/arXiv.1410.5620
5. S. Capitani, Lattice perturbation theory, *Phys. Rep.*, **382** (2003), 113–302.
6. D. M. Blei, M. I. Jordan, *Variational methods for the Dirichlet process*, In: Proceedings of the twenty-first international conference on machine learning, 2004. https://doi.org/10.1145/1015330.1015439
7. K. J. Burns, G. M. Vasil, J. S. Oishi, D. Lecoanet, B. P. Brown, Dedalus: A flexible framework for numerical simulations with spectral methods, *Phys. Rev. Res.*, **2** (2020), 023068. https://doi.org/10.48550/arXiv.1905.10388
8. S. Yasin, A. Khan, S. Ahmad, M. S. Osman, New exact solutions of (3+1)-dimensional modified KdV–Zakharov–Kuznetsov equation by Sardar-subequation method, *Opt. Quant. Electron.*, **56** (2024), 90. http://dx.doi.org/10.1007/s11082-023-05558-2
9. A. Khan, A. U. Khan, S. Ahmad, Investigation of fractal fractional nonlinear Korteweg–de Vries–Schrödinger system with power-law kernel, *Phys. Scr.*, **98** (2023), 085202. https://doi.org/10.3390/sym14040739
10. A. Khalifa, H. Ahmed, K. K. Ahmed, Construction of exact solutions for a higher-order stochastic modified Gerdjikov–Ivanov model using the Imetf method, *Phys. Scr.*, **99** (2024). https://doi.org/10.1088/1402-4896/ada321
11. T. Aktosun, *Inverse scattering transform and the theory of solitons*, Springer, New York, 2022, 47–61. https://doi.org/10.1007/978-1-0716-2457-9_295
12. J. Hietarinta, *Introduction to the Hirota bilinear method*, Springer, Berlin, Heidelberg, 2007, 95–103. https://doi.org/10.1007/BFb0113694
13. J. Blanchet, X. Chen, Steady-state simulation of reflected Brownian motion and related stochastic networks, *Ann. Appl. Probab.*, **25** (2015), 3209–3250. https://doi.org/10.1214/14-AAP1072
14. Y. A. Madani, K. S. Mohamed, S. Yasin, S. Ramzan, K. Aldwoah, M. Hassan, Exploring novel solitary wave phenomena in Klein–Gordon equation using ϕ^6 model expansion method, *Sci. Rep.*, **15** (2025), 1834. http://dx.doi.org/10.1038/s41598-025-85461-w
15. W. A. Faridi, Z. Myrzakulova, R. Myrzakulov, A. Akgül, M. S. Osman, The construction of exact solution and explicit propagating optical soliton waves of Kuralay equation by the new extended direct algebraic and Nucci's reduction techniques, *Int. J. Model. Simul.*, 2024, 1–20. http://dx.doi.org/10.1080/02286203.2024.2326398

16. S. H. Alfalqi, M. M. A. Khater, Numerical solutions and analytical methods for the Kuralay equation: A path to understanding integrable systems, *Opt. Quant. Electron.*, **56** (2024), 756. http://dx.doi.org/10.1007/s11082-024-06597-z
17. W. A. Faridi, M. A. Bakar, Z. Myrzakulova, R. Myrzakulov, A. Akgül, S. M. El Din, The formation of solitary wave solutions and their propagation for Kuralay equation, *Results Phys.*, **52** (2023), 106774. https://doi.org/10.1016/j.rinp.2023.106774
18. M. Iqbal, D. Lu, A. R. Seadawy, N. E. Alsubaie, Z. Umurzakhova, R. Myrzakulov, Dynamical analysis of exact optical soliton structures of the complex nonlinear Kuralay-II equation through computational simulation, *Mod. Phys. Lett. B*, **38** (2024), 2450367. https://doi.org/10.1142/S0217984924503676
19. Beenish, A. K. Alsharidi, Dynamical analysis of exact optical soliton structures of the complex nonlinear Kuralay-II equation through computational simulation, *Mod. Phys. Lett. B*, **38** (2025), 2450512. https://doi.org/10.1142/S0217984924503676
20. N. Cheemaa, H. M. A. Siddiqui, A. Bekir, Stability, sensitivity, chaotic behavior, and phase trajectories evaluation of the Davey-Stewartson stochastic equation, *Nonlinear Dyn.*, **113** (2025), 1102–1118. https://doi.org/10.1007/s11071-025-10912-y
21. S. Ahmad, S. F. Aldosary, M. A. Khan, Stochastic solitons of a short-wave intermediate dispersive variable (SIdV) equation, *AIMS Math.*, **9** (2024), 10717–10733. http://dx.doi.org/2010.3934/math.2024525
22. R. F. Zhang, S. Bilige, Bilinear neural network method to obtain the exact analytical solutions of nonlinear partial differential equations and its application to *p*-gBKP equation, *Nonlinear Dyn.*, **95** (2019), 3041–3048. https://doi.org/10.1007/s11071-018-04739-z
23. S. T. Mohyud-Din, M. A. Noor, Homotopy perturbation method for solving partial differential equations, *Z. Naturforsch. A*, **64** (2009), 157–170. http://dx.doi.org/10.1515/zna-2009-3-402
24. K. S. Nisar, O. A. Ilhan, S. T. Abdulazeez, J. Manafian, S. A. Mohammed, M. S. Osman, Novel multiple soliton solutions for some nonlinear PDEs via multiple Exp-function method, *Results Phys.*, **21** (2021), 103769. https://doi.org/10.1016/j.rinp.2020.103769
25. J. Sun, Auxiliary equation method for solving nonlinear partial differential equations, *Phys. Lett. A*, **309** (2003), 387–396. https://doi.org/10.1016/S0375-9601(03)00196-8
26. S. E. Sherer, J. N. Scott, High-order compact finite-difference methods on general overset grids, *J. Comput. Phys.*, **210** (2005), 459–496. https://doi.org/10.1016/j.jcp.2005.04.017
27. P. R. Kundu, M. R. A. Fahim, M. E. Islam, M. A. Akbar, The sine-Gordon expansion method for higher-dimensional NLEEs and parametric analysis, *Heliyon*, **7** (2021), e06498. https://doi.org/10.1016/j.heliyon.2021.e06459
28. P. Xu, H. Huang, H. Liu, Semi-domain solutions to the fractal (3+1)-dimensional Jimbo–Miwa equation, *Fractals*, **32** (2024), 2450150. https://doi.org/10.1142/S0218348X24400425
29. K. J. Wang, S. Li, Complexiton, complex multiple kink soliton and rational wave solutions to the generalized (3+1)-dimensional Kadomtsev–Petviashvili equation, *Phys. Scr.*, **99** (2024), 075214. http://dx.doi.org/10.1088/1402-4896/ad5062
30. A. Tian, W. Zhang, J. Hei, Y. Hua, X. Liu, J. Wang, et al., Resistance reduction method for building transmission and distribution systems based on an improved random forest model: A tee case study, *Build. Environ.*, 2025, 113256. https://doi.org/10.1016/j.buildenv.2025.113256

31. K. Liu, M. Feng, W. Zhao, J. Sun, W. Dong, Y. Wang, et al., Pixel-level noise mining for weakly supervised salient object detection, *IEEE Trans. Neural Netw. Learn. Syst.*, 2025. https://doi.org/10.1109/TNNLS.2025.3575255
32. P. N. Ryabov, D. I. Sinelshchikov, M. B. Kochanov, Application of the Kudryashov method for finding exact solutions of high-order nonlinear evolution equations, *Appl. Math. Comput.*, **218** (2011), 3965–3972. https://doi.org/10.1016/j.amc.2011.09.027
33. S. Yasin, M. A. Khan, S. Ahmad, S. F. Aldosary, Abundant new optical solitary waves of paraxial wave dynamical model with Kerr media via new extended direct algebraic method, *Opt. Quant. Electron.*, **56** (2024), 925. https://doi.org/10.1007/s11082-024-06845-2
34. M. A. S. Murad, M. A. Mustafa, U. Younas, H. Emadifar, A. S. Khalifa, W. W. Mohammed, et al., Soliton solutions to the generalized derivative nonlinear Schrödinger equation under the effect of multiplicative white noise and conformable derivative, *Sci. Rep.*, **15** (2025), 19599. http://dx.doi.org/10.1038/s41598-025-04981-7
35. B. Øksendal, *Stochastic differential equations: An introduction with applications*, 6 Eds., Springer, Berlin, 2003. https://doi.org/10.1007/978-3-662-13050-6_5
36. N. Raza, A. Javid, Dynamics of optical solitons with Radhakrishnan–Kundu–Lakshmanan model via two reliable integration schemes, *Optik*, **178** (2019), 557–566. https://doi.org/10.1016/J.IJLEO.2018.09.133
37. M. Tariq, M. Moneeb, M. B. Riaz, S. S. Kazmi, M. A. ur Rehman, Unveiling chaos and stability in advection diffusion reaction systems via advanced dynamical and sensitivity analysis, *Sci. Rep.*, **15** (2025), 5513. https://doi.org/10.1038/s41598-025-89995-x
38. M. Tariq, M. Moneeb, M. B. Riaz, T. Kozubek, M. Aziz-ur-Rehman, Exploring chaos and stability: Dynamic insights into the stochastic Davey–Stewartson system through advanced sensitivity analysis, *Model. Earth Syst. Environ.*, **11** (2025), 83. https://doi.org/10.1007/s40808-024-02229-3
39. M. B. Riaz, M. M. Tariq, S. S. Kazmi, M. Aziz-ur-Rehman, Exploring nonlinear dynamics and stability of embedded carbon nanotubes in mechanical engineering, *Arch. Comput. Method. Eng.*, (2025), 1–27. https://doi.org/10.1007/s11831-025-10289-6
40. A. Khalifa, H. Ahmed, K. K. Ahmed, Construction of exact solutions for a higher-order stochastic modified Gerdjikov–Ivanov model using the Imetf method, *Phys. Scr.*, **99** (2024). http://dx.doi.org/10.1088/1402-4896/ada321
41. M. M. Tariq, M. B. Riaz, M. A. ur Rehman, Dilawaiz, Unraveling the complexity of solitary waves in the Klein–Fock–Gordon equation: Dynamical insights into bifurcation and chaos analysis, *Model. Earth Syst. Environ.*, **11** (2025), 51. https://doi.org/10.1007/s40808-024-02249-z
42. H. U. Rehman, S. Yasin, I. Iqbal, Optical soliton for (2+1)-dimensional coupled integrable NLSE using Sardar-subequation method, *Mod. Phys. Lett. B*, **38** (2024), 2450044. https://doi.org/10.1142/S0217984924500441
43. N. Raza, M. A. Ullah, A comparative study of heat transfer analysis of fractional Maxwell fluid by using Caputo and Caputo–Fabrizio derivatives, *Can. J. Phys.*, **98** (2020), 89–101. https://doi.org/10.1139/cjp-2018-0602
44. S. Yasin, F. S. Alshammari, A. Khan, Beenish, Quasi-periodic dynamics and wave solutions of the Ivancevic option pricing model using multi-solution techniques, *Symmetry*, **17** (2025), 1137. https://doi.org/10.3390/sym17071137

45. N. Raza, I. G. Murtaza, S. Sial, M. Younis, On solitons: The biomolecular nonlinear transmission line models with constant and time-variable coefficients, *Wave. Random Complex*, **28** (2018), 553–569. https://doi.org/10.1080/17455030.2017.1368734
46. M. E. Ramadan, H. M. Ahmed, A. S. Khalifa, K. K. Ahmed, Analytical study of fractional solitons in three dimensional nonlinear evolution equation within fluid environments, *Sci. Rep.*, **15** (2025), 35399. http://dx.doi.org/10.1038/s41598-025-12576-5

AIMS Press